

We are IntechOpen, the world's leading publisher of Open Access books Built by scientists, for scientists

4,800

Open access books available

122,000

International authors and editors

135M

Downloads

Our authors are among the

154

Countries delivered to

TOP 1%

most cited scientists

12.2%

Contributors from top 500 universities



WEB OF SCIENCE™

Selection of our books indexed in the Book Citation Index
in Web of Science™ Core Collection (BKCI)

Interested in publishing with us?
Contact book.department@intechopen.com

Numbers displayed above are based on latest data collected.

For more information visit www.intechopen.com



ZnO-Based Light-Emitting Diodes

J.C. Fan, S.L. Chang and Z. Xie

Additional information is available at the end of the chapter

<http://dx.doi.org/10.5772/51181>

1. Introduction

In the past decade, light-emitting diodes (LEDs) based on wideband gap semiconductor have attracted considerable attention due to its potential optoelectronic applications in illumination, mobile appliances, automotive and displays [1]. Among the available wide band gap semiconductors, zinc oxide, with a large direct band gap of 3.37eV, is a promising candidate because of characteristic features such as a large exciton binding energy of 60meV, and the realization of band gap engineering to create barrier layers and quantum wells with little lattice mismatch. ZnO crystallizes in the wurtzite structure, the same as GaN, but, in contrast, large ZnO single crystal can be fabricated [2]. Furthermore, ZnO is inexpensive, chemically stable, easy to prepare and etch, and nontoxic, which also make the fabrication of ZnO-based optical devices an attractive prospect. The commercial success of GaN-based optoelectronic and electronic devices trig the interest in ZnO-based devices [2-4].

Recently, the fabrication of *p*-type ZnO has made great progress by mono-doping group V elements (N, P, As, and Sb) and co-doping III-V elements with various technologies, such as ion implantation, pulsed laser deposition (PLD), molecular beam epitaxy (MBE) [2,3]. A number of researchers have reported the development of homojunction ZnO LEDs and heterojunction LEDs using *n*-ZnO deposited on *p*-type layers of GaN, AlGaIn, conducting oxides, or *p*-ZnO deposited on a *n*-type layer of GaN [1,3].

Figure1a shows the schematic structure of a typical ZnO homostructural p-i-n junction prepared by Tsukaza et al [5]. The I-V curve of the device displayed the good rectification with a threshold voltage of about 7V (Figure1b). The electroluminescence (EL) spectrum from the p-i-n junction (blue) and photoluminescence (PL) spectrum of a p-type ZnO film at 300K were shown in Figure1c, which indicated that ZnO was a potential material for making short-wavelength optoelectronic devices, such as LEDs for display, solid-state illumination and photodetector.

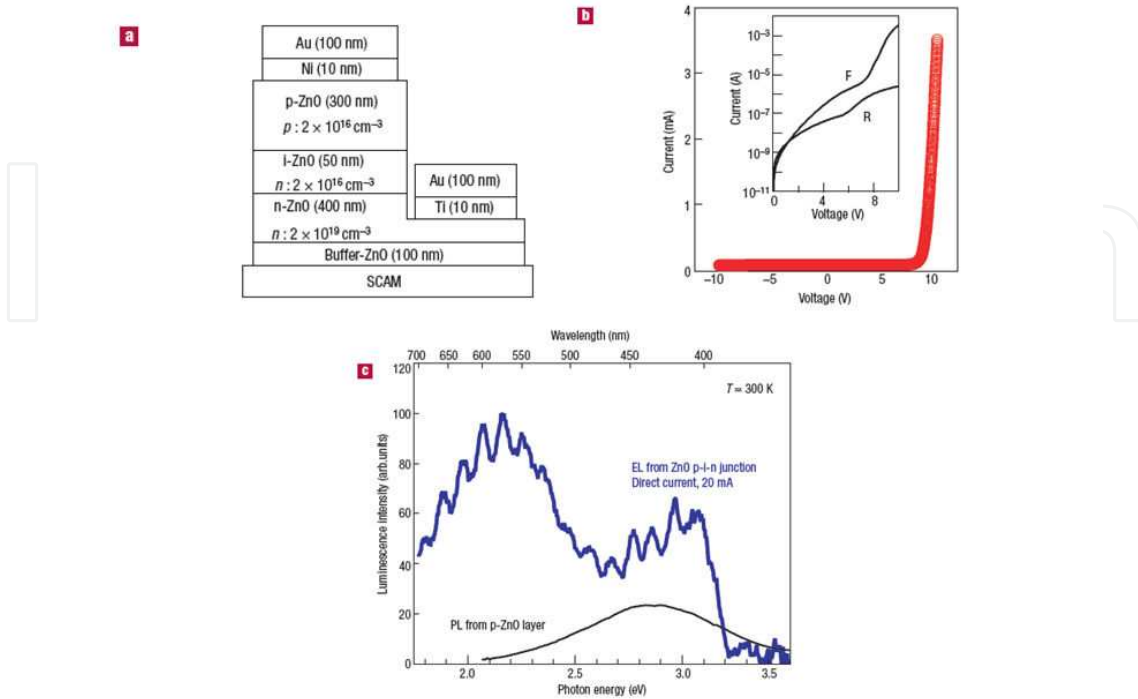


Figure 1. ZnO homostructural p-i-n junction shows rectifying current-voltage characteristics and electroluminescence (EL) in forward bias at room-temperature. (a), The structure of a typical p-i-n junction LED. (b), Current-voltage characteristics of a p-i-n junction. The inset has logarithmic scale in current with F and R denoting forward and reverse bias conditions, respectively. (c), Electroluminescence spectrum from the p-i-n junction (blue) and photoluminescence (PL) spectrum of a p-type ZnO film measured at 300 K. The p-i-n junction was operated by feeding in a direct current of 20 mA. From Ref.[5].

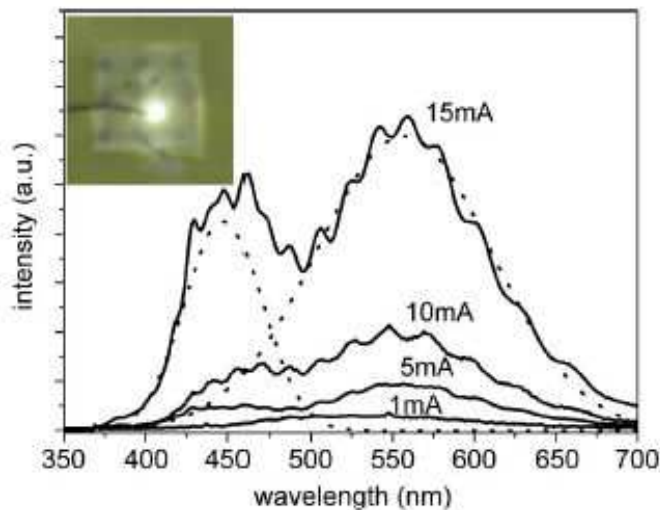


Figure 2. Room-temperature EL spectra of the n-ZnO/p-GaN heterojunction LED measured at various dc injection currents from 1 to 15mA at reverse breakdown biases. (Inset) EL image of the LED in a bright room. From Ref. [6].

White-light electroluminescence from n-ZnO/p-GaN heterojunction LED was reported [6]. The spectrum range from 400 to 700nm is caused by the carrier recombination at the interface between n-ZnO and p-GaN, as shown in Figure2, which makes ZnO as a strong candidates for solid-state light.

Currently, ZnO-based LEDs are leaping from lab to factory. A dozen or so companies are developing ultraviolet and white LEDs for market. The coloured ZnO-based LEDs have been produced by Start-up company MOXtronics, which shows its full-colour potential. Although the efficiency of these LEDs is not high, improvements are rapid and the emitters have the potential to outperform their GaN rivals. Figure3 shows some EL images of ZnO-based LEDs.

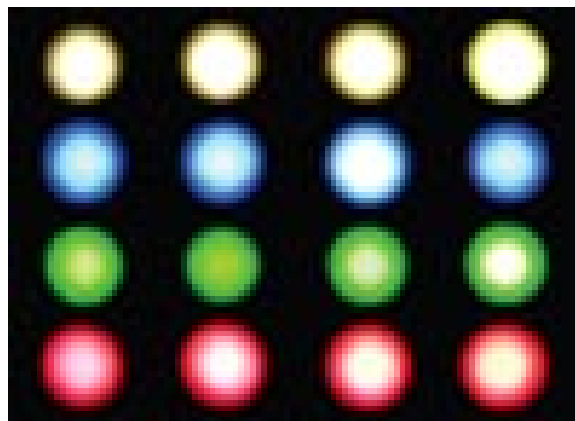


Figure 3. Some EL images of ZnO-based LEDs. From Ref. [7].

In this paper, based on the introduction of the band-gap engineering and doping in ZnO, we discuss the ZnO-based LEDs, comprehensively. We first discuss the band-gap engineering in ZnO, which is a very important technique to design ZnO-based LEDs. We then present the p- and n-types doping in ZnO. High quality n-type and/or p-type ZnO are necessary to prepare ZnO-based LEDs. Finally, we review the ZnO-based LEDs. In this part, we discuss homojunction ZnO LEDs and heterojunctions LEDs using *n*-ZnO deposited on *p*-type layers (GaN, AlGaN, conducting oxides, et al) or *p*-ZnO deposited on a *n*-type layer (GaN, Si, et al), comprehensively.

2. Band gap engineering in ZnO

Band gap engineering is the process of controlling or altering the band gap of a material by controlling the composition of certain semiconductor alloys. It is well known that tailoring of the energy band gap in semiconductors by band-gap engineering is important to create barrier layers and quantum wells with matching material properties, such as lattice constants, electron affinity for heterostructure device fabrication [2, 3].

Band-gap engineering in ZnO can be achieved by alloying with MgO, CdO or BeO. The energy band gap $E_g(x)$ of ternary semiconductor $A_xZn_{1-x}O$ ($A = \text{Mg, Cd or Be}$) can be calculated by the following equation:

$$E_g(x) = (1-x) E_{ZnO} + x E_{AO} - bx(1-x) \quad (1)$$

where b is the bowing parameter and E_{AO} and E_{ZnO} are the band-gap energies of compounds AO and ZnO, respectively. While adding Mg or Be to ZnO results in an increase in band gap, and adding Cd leads to a decrease in band gap [3, 8].

Both MgO and CdO have the rock-salt structure, which is not the same as the ZnO wurtzite structure. When Mg and Cd contents in ZnO are high, phase separation may be detected, while BeO and ZnO share the same wurtzite structure and phase separation is not observed in BeZnO [2, 8]. Ryu et al studied the band gap of BeZnO and did not observe any phase separation when Be content was varied over the range from 0 to 100mol%. Figure 4 shows the a lattice parameter as a function of room-temperature E_g values in $A_xZn_{1-x}O$ alloy. Therefore, theoretically, the energy band gap of $A_xZn_{1-x}O$ can be continuously modulated from 0.9eV (CdO) to 10.6eV (BeO) by changing the A concentration [8]. Han et al reported the band gap energy of the $Be_xZn_{1-x}O$ can be tailored from 3.30eV ($x = 0$) to 4.13eV ($x = 0.28$) by alloying ZnO with BeO [9].

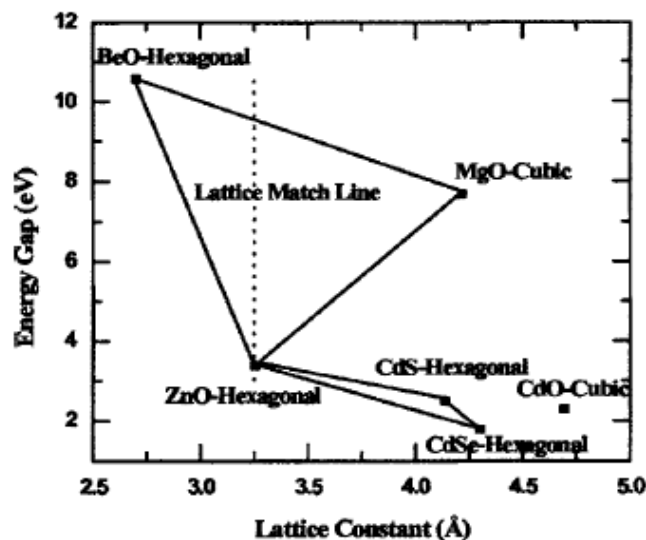


Figure 4. Energy band gaps, lattice constants and crystal structures of selected II-VI compounds. From Ref. [9].

Ohtomo et al investigated the band gap of $Mg_xZn_{1-x}O$ films grown on sapphire by PLD, where x is the atomic fraction [10]. The band gap of $Mg_xZn_{1-x}O$ could be increased to 3.99eV at room temperature as the content of Mg was increased upward to $x = 0.33$. Above 33%, the phase segregation of MgO impurity was observed from the wurtzite MgZnO lattice. Takagi et al reported the growth of wurtzite MgZnO film with Mg concentration of 51% on sapphire by molecular-beam epitaxy [11]. The band gap energy of $Mg_xZn_{1-x}O$ was successfully

turned from 3.3 to 4.5eV with the increase of Mg contents from 0 to 0.5. Tampo et al investigated excitonic optical transition in a $\text{Zn}_{1-x}\text{Mg}_x\text{O}$ alloy grown by radical source molecular beam epitaxy [12]. The strong reflectance peaks at room temperature were detected from 3.42eV ($x=0.05$) to 4.62eV ($x = 0.61$) from ZnMgO layers at room temperature. PL spectra at room temperature were also observed for energies up to 4.06eV ($x = 0.44$). Wassner et al studied the optical and structural properties of MgZnO films with Mg contents between $x = 0$ and $x = 0.37$ grown on sapphire by plasma assisted molecular beam epitaxy using a MgO/ZnMgO buffer layer [13]. In their experiments, the *a*-lattice parameter was independent from the Mg concentration, whereas the *c*-lattice parameter decreases from 5.20Å for $x = 0$ to 5.17Å for $x = 0.37$, indicating pseudomorphic growth. The peak position of the band edge luminescence blue shifted up to 4.11eV for $x = 0.37$.

Makino et al investigated the structure and optical properties of $\text{Cd}_x\text{Zn}_{1-x}\text{O}$ films grown on sapphire (0001) and ScAlMgO_4 substrates by PLD [14]. The band gap of $\text{Cd}_x\text{Zn}_{1-x}\text{O}$ films was estimated by $E_g(y) = 3.29 - 4.40y + 5.93y^2$. The band gap narrowing to 2.99eV was achieved by incorporating Cd^{2+} with Cd concentration of 7%. Both lattice parameters *a* and *c* increase with the increasing Cd content in ZnO, which was agreement with the larger atomic size of Cd compared with Zn. $\text{Cd}_x\text{Zn}_{1-x}\text{O}$ films were also prepared on *c*-plane sapphires by metal-organic vapor-phase epitaxy. The fundamental band gap was narrowed up to 300meV for a maximum Cd concentration of ~5%, introducing a lattice mismatch of only 0.5% with respect to binary ZnO. Lai et al prepared the $\text{Cd}_x\text{Zn}_{1-x}\text{O}$ alloy by conventional solid-state reaction over the composition range and found that CdO effectively decreased the electronic bandgap both in the bulk and near the surface ZnO [15].

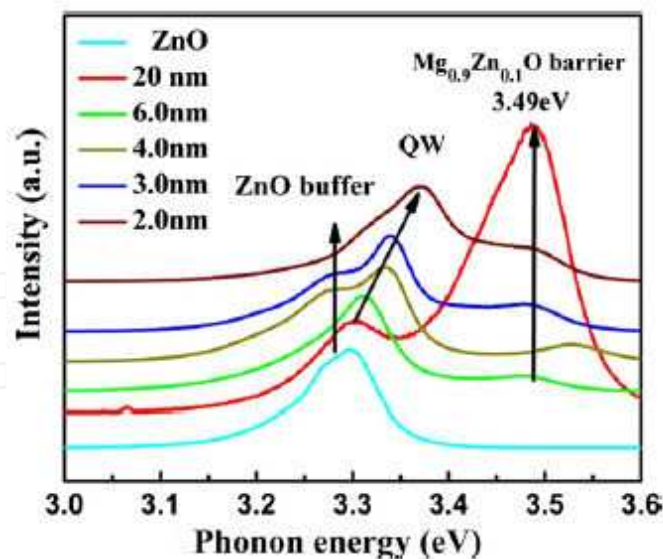


Figure 5. Room temperature PL spectra of ZnO/ $\text{Zn}_{0.9}\text{Mg}_{0.1}\text{O}$ SQW with different well width. From Ref. [17].

Using MgZnO as barrier layers, Chauveau et al prepared the nonpolar *a*-plane (Zn,Mg)O/ZnO quantum wells (QWs) grown by molecular beam epitaxy on *r* plane sapphire and *a* plane ZnO substrates [16]. They observed the excitonic transitions were strongly blue-shifted due to the

anisotropic strain state in heteroepitaxial QW and the reduction of structural defects and the improvement of surface morphology were correlated with a strong enhancement of the photoluminescence properties. Su et al investigated the optical properties of ZnO/ZnMgO single quantum well (SQW) prepared by plasma-assisted molecular beam epitaxy [17]. The photoluminescence peak of the SQW shifted from 3.31 to 3.37eV as the well layer thickness was decreased from 6 to 2nm (Figure5). ZnO/MgZnO superlattices were also fabricated by laser molecular-beam epitaxy and the excitonic stimulated emission up to 373K was observed in the superlattices. The emission energy could be tuned between 3.2 and 3.4eV, depending on the well thickness and/or the Mg content in the barrier layers.

3. Doping in ZnO

ZnO has a strong potential for various short-wavelength optoelectronic device applications. To realize these applications, the reliable techniques for fabricating high quality n-type and p-type ZnO need to be established. Undoped ZnO exhibits n-type conduction due to the intrinsic defects, such as the Zinc interstitial (Zn_i) and oxygen vacancy (V_o). It is easy to obtain the high quality n-type ZnO material by doping group-III elements. However, it is a major challenge to dope ZnO to produce p-type semiconductor due to self-compensation from native donor defects and/or hydrogen incorporation. To achieve p-type ZnO, various elements (N, P, As, Sb and Li) have been tried experimentally as p-type dopants with various techniques, such as pulse laser deposition, magnetron sputtering, chemical vapor deposition (CVD), molecular-beam epitaxy, hybrid beam deposition (HBD), metal organic chemical vapor deposition (MOCVD) and thermal oxidation of Zn_3N_2 [2, 3].

3.1. n-type ZnO

A number of researchers investigated the electrical and optical properties of n-type ZnO materials by doping III elements, such as Al, Ga and In, which can easily substitute Zn ions [1-3].

Kim et al reported the high electron concentration and mobility in AZO films grown on sapphire by magnetron sputtering [18]. AZO films exhibited the electron concentrations and mobilities were of the order of $10^{18}cm^3$ and less than $8cm^2/Vs$, respectively, however, when annealed at $900^{\circ}C$, the films showed remarkably improved carrier concentrations and mobilities, e.g., about $10^{20}cm^3$ and $45 - 65 cm^2/Vs$, respectively. Other researchers also reported the improved electrical properties in Al-doped zinc oxide by thermal treatment [19].

Bhosle et al investigated the electrical properties of transparent Ga-doped ZnO films prepared by PLD [20]. Temperature dependent resistivity measurements for the films showed a metal-semiconductor transition, which was rationalized by localization of degenerate electrons. The lowest value of resistivity $1.4 \times 10^{-4} \Omega cm$ was found at 5% Ga. Yamada et al reported the low resistivity Ga-doped ZnO films prepared on glass by ion plating with direct current arc discharge [21]. The ZnO:Ga film with a thickness of 98nm, exhibited a resistivity of $2.4 \times 10^{-4} \Omega cm$, a carrier concentration of $1.1 \times 10^{21}cm^{-3}$ and a Hall mobility of $23.5cm^2/Vs$. Liang et al reported the Ga-doped ZnO films prepared on

glass by magnetron sputtering and found that a carrier concentration exhibited only a slight change with the thickness variations [22].

Wang et al studied the properties of In-doped ZnO crystal by the hydrothermal technique [23]. The indium-doped ZnO crystals have a resistivity lower than $0.015\Omega\text{cm}$ with a free carrier concentration (mostly due to indium donors) of $1.09\times 10^{19}/\text{cm}^3$ at room temperature. Quang et al reported the In-doped ZnO films grown by hydrothermal [24]. The films had a mobility of $4.18\text{--}20.9\text{cm}^2/\text{Vs}$ and a concentration of $6.7\times 10^{18} - 3.2\times 10^{19}/\text{cm}^3$. The In-doped ZnO films with a carrier concentration of $3.22\times 10^{20}/\text{cm}^3$ were grown by sol-gel method [25].

VII elements such as F and Cl are also used as n-type dopants in ZnO, which substituted oxygen ions. Cao et al reported F-doped ZnO grown by PLD with a minimum resistivity of $4.83\times 10^{-4}\Omega\text{cm}$, with a carrier concentration of $5.43\times 10^{20}\text{cm}^{-3}$ and a mobility of $23.8\text{cm}^2/\text{Vs}$ [26]. Chikoidze et al grew Cl-doped ZnO films by MOCVD with a resistivity of $3.6\times 10^{-3}\Omega\text{cm}$ [27].

3.2. p-type ZnO

To realize ZnO-based LEDs, the most important issue is the fabrication of high quality p-type ZnO. However, undoped ZnO exhibits n-type conduction and the reliable p-type doping of the materials remains a major challenge because of the self-compensation from native donor defects (V_O and Zn_i) and/or hydrogen incorporation. Considerable efforts have been made to obtain p-type ZnO by doping different elements (N, P, As, Sb, Li, Na and K) with various techniques [2, 3]. Here, we present the typical results of p-type ZnO materials.

Among all potential p-type dopants for ZnO, N is considered the most promising dopant due to similar ionic radius compared with oxygen. It substitutes O sites in ZnO structure, resulting in the shallow acceptors. N_2 , NO, N_2O , NH_3 and Zn_3N_2 are acted as N sources depended on growth techniques [2, 3]. Liu et al reported p-type ZnO:N films grown on c-sapphire by plasma-assisted molecular beam epitaxy [28]. The anomalous Raman mode at 275cm^{-1} was confirmed to be related to substitution of N for O site (N_O) in ZnO. The films exhibited a hole concentration of $2.21\times 10^{16}\text{cm}^{-3}$ and a mobility of $1.33\text{cm}^2/\text{Vs}$. Zeng et al investigated p-type ZnO films prepared on a-plane (11-20) sapphire by MOCVD [29]. The optimized result was achieved at the temperature of 400°C with a resistivity of $1.72\Omega\text{cm}$, a Hall mobility of $1.59\text{cm}^2/\text{Vs}$, and a hole concentration of $2.29\times 10^{18}\text{cm}^{-3}$. Wang et al prepared p-type ZnO films by oxidation of Zn_3N_2 films grown by direct current magnetron sputtering [30]. For oxidation temperature between 350 and 500°C , p-type ZnO:N films were achieved, with a hole concentration of $5.78\times 10^{17}\text{cm}^{-3}$ at 500°C . Kumar et al reported on the growth of p-type N,Ga-codoped ZnO films prepared by sputtering ZnO:Ga₂O₃ target in N_2O ambient [31]. The film deposited on sapphire at 550°C exhibited p-type conduction with a hole concentration of $3.9\times 10^{17}\text{cm}^{-3}$.

Beside N, other group V elements (P, As and Sb) are also used to be acceptor dopants to obtain p-type ZnO. However, first-principle calculations show that X_O (P_O , As_O and Sb_O) are deep acceptors and have high acceptor-ionization energies, owing to their large ionic radii as compared to O, which make it impossible for X_O to dop ZnO efficiently p-type [32]. We

could not contribute the p-type behaviour in X doped ZnO to X_{O} , simply. Recently, for the large-size-mismatched impurities in ZnO, Limpijumng et al proposed $X_{\text{Zn}}-2V_{\text{Zn}}$ acceptor model [33]. In the model, X substitute Zn sites, forming a donor, then it induces two Zn vacancy acceptors as a complex form $X_{\text{Zn}}-2V_{\text{Zn}}$. The ionization energy of $\text{As}_{\text{Zn}}-2V_{\text{Zn}}$ complex was calculated to be 0.15eV (0.16eV for $\text{Sb}_{\text{Zn}}-2V_{\text{Zn}}$).

Xiu et al reported p-type P-doped ZnO films grown by MBE using a GaP effusion cell as a phosphorus dopant source [34]. PL spectra clearly indicated the existence of competitions between D^0X and A^0X for the phosphorus-doped ZnO films. The films exhibited a carrier concentration of $6.0 \times 10^{18} \text{ cm}^{-3}$, Hall mobility of $1.5 \text{ cm}^2/\text{Vs}$, and resistivity of $0.7 \Omega\text{cm}$. Kim et al achieved p-type ZnO:P films on a sapphire substrate using phosphorus doping and a thermal annealing process [35]. As-grown n-type ZnO:P prepared by radio-frequency sputtering were converted to p-ZnO:P by an rapid thermal annealing process under a N_2 ambient. The films had a hole concentration of $1.0 \times 10^{17} - 1.7 \times 10^{19}/\text{cm}^3$, a mobility of $0.53 - 3.51 \text{ cm}^2/\text{Vs}$ and a resistivity of $0.59 - 4.4 \Omega\text{cm}$. Pan et al prepared p-type ZnO:P films on the insulating quartz with a hole concentration of $1.84 \times 10^{18} \text{ cm}^{-3}$ by MOCVD [36]. Vaithianathan et al grew p-type ZnO:P films on $\text{Al}_2\text{O}_3(0001)$ by PLD [37]. The films exhibited a hole concentration of $5.1 \times 10^{14} - 1.5 \times 10^{17} \text{ cm}^{-3}$, a hole mobility of $2.38 - 39.3 \text{ cm}^2 / \text{V s}$, and a resistivity of $17 - 330 \Omega\text{cm}$.

Ryu et al investigated the electrical properties of As-doped ZnO films on O-ZnO substrates by hybrid beam deposition [38]. The electrical behavior of ZnO:As films changed from intrinsic n-type to highly conductive p-type with increased As dopant concentration. They achieved p-type ZnO:As films with a hole concentration of $4 \times 10^{17} \text{ cm}^{-3}$ and a mobility of $35 \text{ cm}^2/\text{Vs}$. Vaithianathan et al reported As-doped p-type ZnO films using a $\text{Zn}_3\text{As}_2/\text{ZnO}$ target by PLD [39]. As-grown ZnO:As showed n-type conductivity, however, ZnO:As films after annealed at 200°C in N_2 ambient for 2 min exhibited p-type conductivity with the hole concentrations varied between 2.48×10^{17} and $1.18 \times 10^{18} \text{ cm}^{-3}$. Kang et al grew ZnO films on GaAs by sputtering and annealed at 500°C in an oxygen gas pressure of 40 mTorr for 20 min. After annealing, ZnO film on GaAs showed p-type conductivity with a hole concentration of $9.684 \times 10^{19} \text{ cm}^{-3}$, a mobility of $25.37 \text{ cm}^2/\text{Vs}$, and a resistivity of $2.54 \times 10^{-3} \Omega\text{cm}$. The acceptor binding energy was calculated to be 0.1445eV, which was in good agreement with the ionization energy of $\text{As}_{\text{Zn}}-2V_{\text{Zn}}$ acceptor complex (0.15eV) [40].

Guo et al reported p-type ZnO:Sb films grown by PLD [41]. The films showed a resistivity of $4.2 - 60 \Omega\text{cm}$, a Hall mobility of $0.5 - 7.7 \text{ cm}^2/\text{V s}$, and a hole concentration of $1.9 - 2.2 \times 10^{17} \text{ cm}^{-3}$. In the (HR) TEM images of p-type ZnO:Sb, they observed a high density of threading dislocations originating from the film/substrate interface and a large number of partial dislocation loops associated with small stacking faults. Xiu et al fabricated p-type ZnO:Sb films grown on n-Si (100) by MBE [42]. The film had a concentration of $1.7 \times 10^{18} \text{ cm}^{-3}$, and a high mobility of $20.0 \text{ cm}^2/\text{Vs}$ and a low resistivity of $0.2 \Omega\text{cm}$. The acceptor energy level of the Sb dopant was about 0.2eV above the valence band, which was agreement with the ionization energy of $\text{Sb}_{\text{Zn}}-2V_{\text{Zn}}$ (0.16eV).

Some researchers prepared p-type ZnO using Group I elements (Li, Na and K) as acceptor dopants. Yi et al fabricated p-type ZnO:Li films grown on quartz substrate by PLD

with a hole concentration of $5.4 \times 10^{18} \text{cm}^{-3}$ [43]. p-type ZnO:Na films were fabricated on Si substrates by PLD [44]. The hole concentration ranged from 1.5×10^{18} to $1.1 \times 10^{19} \text{cm}^{-3}$. Wu et al grew K-doped p-type ZnO films on (0001) Al_2O_3 substrates by radio frequency magnetron sputtering [45].

Growth technique	Structure	Light emission (nm)	Reference
	n-ZnO/p-GaN	570	[46]
	n-ZnO/p-GaN	450, 520	[47]
MBE	n-ZnO:Ga/p-GaN:Mg	430	[48]
	n-MgZnO/CdZnO/p-GaN	390, 410	[49]
	n-MgZnO/n-ZnO/p-AlGaIn/p-GaN	390	[50]
	n-ZnO:Ga/p-GaN:Mg	430, 440, 480	[51]
Magnetron sputtering	n-ZnO /p-GaN	400, 400-700	[52]
	n-ZnO:Ga/i-ZnO/p-GaN:Mg	405, 530, 620	[53]
	n-ZnO/AlN/p-GaN:Mg	392	[54]
	n-ZnO:Er/p-GaN:Mg	537, 538	[55]
PLD	p-SrCu ₂ O ₂ /n-ZnO	382	[56]
	n-ZnO/p-GaN:Mg	375	[57]
	n-ZnO/p-GaN:Mg	365.4, 384	[58]
MOCVD	n-ZnO /p-Si	580	[59]
	n-ZnO /p-Si	400-600	[60]
CVD	n-ZnO/p-AlGaIn	389	[61]
	n-ZnO/p-GaN	430	[62]
HWEF sputtering	p-CuGaS ₂ /n-ZnO:Al	496-775	[63]

Table 1. Structure and emission of n-ZnO based LEDs.

4. ZnO-based LEDs

4.1. Heterojunction LEDs

4.1.1. n-ZnO heterojunction LEDs

ZnO has attracted considerable attention because of its promising applications in UV LEDs and laser diodes. The fabrication of high-quality p-type ZnO remains great challenge. Many researchers reported on the heterojunction LEDs with n-type ZnO grown on p-type materials of Si, GaN and conducting oxides, as summarized in Table1.

Chang et al reported the MBE n-ZnO/MOCVD p-GaN heterojunction light-emitting diode [46]. They grew 1- μm -thick undoped GaN buffer layer on Al_2O_3 and a 500-nm-thick Mg-doped p-GaN layer by MOCVD, and grew 300-nm-thick n-ZnO by MBE on p-GaN layer. They observed a broad yellowish green emission peaked at around 570nm. The EL emission was attributed to the electron injection from n-ZnO to p-GaN. Hwang et al fabricated an n-ZnO:Ga/p-GaN:Mg heterostructure on Al_2O_3 substrate [51]. Undoped ZnO (buffer layer) and n-ZnO films doped with about 1% Ga were grown at 75W radio frequency (RF) power in 100% O_2 atmosphere, at 800°C and 700°C, respectively. I-V characteristics exhibited the typical rectifying behavior and the EL emissions from the n-ZnO:Ga/p-GaN:Mg heterostructure at room temperature show peaks at 430nm, 440nm and 480nm along with a broad band of yellow light.

Lee et al investigated the origin of emission of the annealed n-ZnO/p-GaN heterostructure LED [52]. They fabricated n-ZnO/p-GaN heterojunction LED on Al_2O_3 substrates by MOCVD (GaN layer) and RF sputtering (ZnO layer). After fabrication, ZnO films were annealed in a thermal furnace in air and nitrogen ambient at 800°C for 30–120min. For the LED annealed in N_2 , room-temperature EL in the blue region with peak wavelength 400nm was observed, and for the LED annealed in N_2 , a broad band from 400 to 700nm was detected in the EL emission spectrum, as shown in Figure 6. Alivov et al reported the n-ZnO/p-AlGaIn heterojunction light-emitting diodes on 6H-SiC substrates [61]. n-type ZnO layer with a thickness of 1 μm was deposited on p- $\text{Al}_{0.12}\text{Ga}_{0.88}\text{N}$ and I-V curve of the devices showed a rectifying diode-like behavior with threshold voltage ~ 3.2 V, a high reverse breakdown voltage of 30V and a small reverse leakage current of about 10^{-7} A. Under forward bias, UV EL with a peak emission near 389nm ($\sim 3.19\text{eV}$) and a full-width at half-maximum (FWHM) of 26nm was observed in the EL spectrum of the device. The emission was stable at temperatures up to 500K and was attributed to the recombination of the carriers within the ZnO. They also observed 430nm electroluminescence from ZnO/GaN heterojunction LEDs [62]. Yu et al reported ZnO/GaN heterostructure LEDs with a donor-acceptor pair emission band at 3.270eV [58]. In the EL spectrum of the device, two emission peaks, a strong emission peak (384.0nm), together with a weak emission (365.4nm) feature on the higher-energy side.

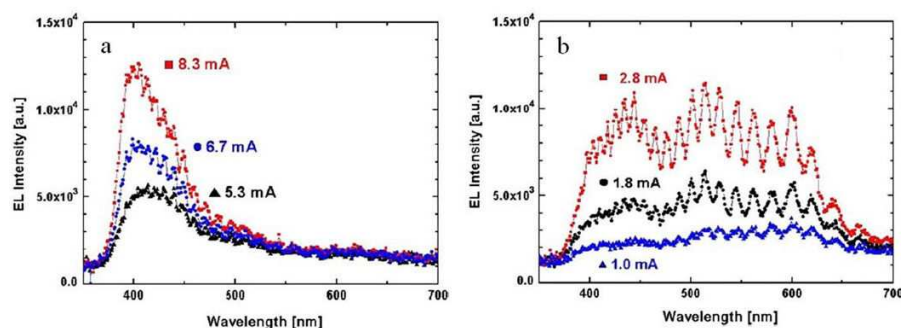


Figure 6. EL spectra of n-ZnO/p-GaN heterostructure LED annealed (a) in N_2 and (b) in air ambient. Inset: pictures of Light emission. From Ref. [52].

Chichibu et al fabricated p-CuGaS₂/n-ZnO:Al heterojunction LEDs by metal-organic vapor phase epitaxy (p-CuGaS₂) and helicon-wave-excited-plasma (HWEP) sputtering method (n-ZnO:Al) [63]. The EL spectra exhibited emission peaks and bands between 1.6 and 2.5eV. Ohta et al reported on p-SrCu₂O₂/n-ZnO heterojunction LEDs [56]. The I-V curve of the device exhibited nonlinear characteristics where the turn-on voltage was approximately 1.5V. An UV emission band centered at 382nm was observed at room temperature when a forward bias voltage greater than 3V was applied to the device, as shown in Figure 7.

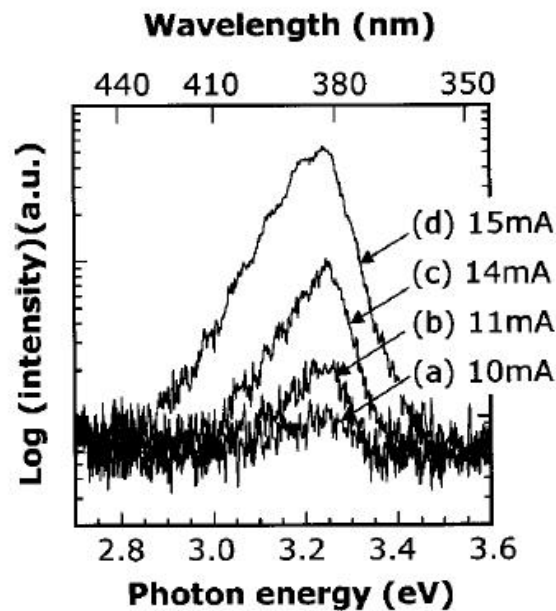


Figure 7. UV emission spectra of the p-SrCu₂O₂ /n-ZnO p – n junction LED for several currents. electric currents were (a) 10mA, (b) 11mA, (c) 14mA, and (d) 15mA, respectively. From Ref. [56].

Ye et al reported the distinct visible electroluminescence at room temperature from n-ZnO/p-Si heterojunction [59]. A high-quality ZnO layers were fabricated by metal organic chemical vapor deposition technique on p-type Si (111) substrate at 650°C. Before grew ZnO layer, a thin ZnO buffer layer (~25nm) was deposited to relieve the strains due to large lattice mismatch between Si and ZnO and to avoid the oxidation of Si surface. The EL peak energy coincided well with the deep-level photoluminescence of ZnO, indicating that the EL emission was originated from the radiative recombination via deep-level defects in n-ZnO layers.

To improve the emission of n-ZnO-based heterojunction LEDs, double and triple heterojunction LEDs were fabricated. Osinsky et al reported MgZnO/ZnO/AlGaN/GaN triple heterostructures light-emitting diodes [50]. I-V curves of the device showed a rectifying characteristics with a turn-on voltage of ~3.2 V. Strong optical emission was observed at ~390nm. Mares et al prepared a hybrid n-MgZnO/CdZnO/p-GaN LEDs with a Cd_{0.12}Zn_{0.88}O quantum-well [49]. Under forward bias, visible electroluminescence was observed at room temperature in the EL spectrum of the device. The EL red shifted from 3.32 to 3.15eV as the

forward current was increased from 20 to 40mA. Zhang et al investigated the effects of the crystalline and thickness of AlN layer on the electroluminescent performance of n-ZnO/AlN/p-GaN [54]. They found that the better crystalline quality of AlN barrier layer may facilitate the improvement of EL performance of the device. For the thinner AlN layer, it was not enough to cover the whole surface of GaN, while in the thicker AlN layer, many of electrons were captured and nonradiatively recombined via the deep donors, indicating that AlN barrier layer played an important role on the performance of the device. In their experiments, AlN layer at the growth temperature of 700°C with an optimized thickness of around 10nm improved EL performance of the devices.

4.1.2. Heterojunction LEDs with ZnO nanomaterials

The optical devices using ZnO nanomaterials have attracted considerable attention due to their promising optical properties, such as enriched radiative recombination of carriers. Various ZnO nanomaterials have been grown by different methods. Based on the growth of n-type ZnO nanomaterials, some researcher reported the heterojunction LEDs with ZnO nanomaterials, as summarized in Table 2. Here, we only present the typical results on heterojunction LEDs with ZnO nanomaterials.

Growth technique	Structure	Light emission (nm)	Reference
Solution method	n-ZnO nanowire/p-GaN film	400-420	[64]
	n-ZnO nanorods/PFO	448, 469, 503, 541, 620	[65]
	n-ZnO nanowire/i-polymer/p-GaN	400	[66]
	n-ZnO (nanowall, nanorod, nanoflower, nanotube) /p-GaN	White light	[67]
	n-ZnO nanorod/polymer	420-800	[68]
CVD	n-ZnO nanowire/p-GaN film	370, 400- 440	[69]
	n-ZnO nanowire in polystyrene /PEDOT:PSS	383,430,640,748	[70]
	n-ZnO nanowire/p-Si	600	[71]
	ITO/n-ZnO nanorod/p ⁺ -Si	450	[72]
MOCVD	n-ZnO nanorod/p-GaN film	370, 440, 560	[73]
	n-ZnO nanorod/p-GaN film	440-560	[74]
Electrodeposition	n-ZnO nanowire/p-GaN film	397	[75]
	n-ZnO nanorod/p-CuSCN	390	[76]
	p-NiO film /n-ZnO nanorod	UV-visible	[77]
PLD	n-ZnO nanowire/p-GaN film	380	[78]

Table 2. Structure and emission of heterojunction LEDs with ZnO nanostructures.

Xu et al reported ordered ZnO nanowire array blue/near-UV LEDs [64]. The devices were fabricated by a conjunction of low temperature wet chemical methods and electron beam lithography. ZnO nanowire arrays were grown on Mg-doped p-type GaN films. $I - V$ curves of the devices exhibited the typical rectifying behavior. Under forward bias, each single nanowire was a light emitter. The EL spectra of the devices were shown in Figure 8. It can be seen that the contour of the EL spectrum does not change much with the biased voltage in the range of 4-10V and the dominant emission peak is slightly blue shifted in the range of 400nm– 420nm. By Gaussian deconvolution of the emission spectrum, the blue/near-UV emission is attributed particularly to three distinct electron-hole recombination processes. The LEDs give an external quantum efficiency of 2.5%, displaying great potential applications in high resolution electronic display, optical interconnect, and high density data storage.

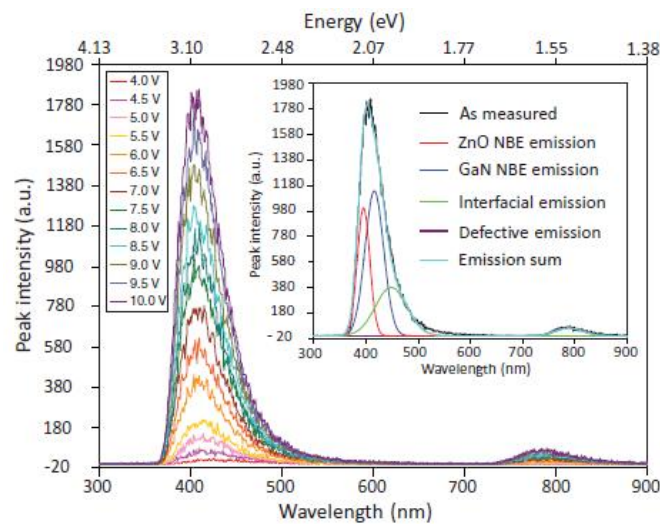


Figure 8. EL spectrum as a function of the forward biased voltage. Inset shows by Gaussian deconvolution analysis the blue/near-UV emission could be decomposed into three distinct bands that correspond to three different optoelectronic processes. From Ref. [64].

Zhang et al fabricated high-brightness blue-light-emitting diode using a ZnO-nanowire array grown on p-GaN thin film [69]. The EL spectrum of the device showed broad emission peaks from UV (370nm) to blue. When the forward bias increased from 10 to 35V, the emission peak was significantly enhanced and the main emission peak shifted from 440 to 400nm when the forward bias was increased (Figure 9), indicating that the modification of external voltage to the band profile in the depletion region. Lupan et al observed UV emission at 397nm with a low forward-voltage emission threshold of 4.4V and a high brightness above 5– 6V in ZnO-nanowire/p-GaN LEDs [75].

Alvi et al investigated the n-ZnO nanostructures (nanowalls, nanorods, nanoflowers and nanotubes)/p-GaN white-light-emitting diodes, systematically [67]. In their experiments, ZnO nanostructures were grown on p-GaN substrates using a low temperature aqueous chemical growth method (<100°C) forming p – n heterojunctions. The EL spectrum of ZnO-

nanowall LED exhibited three peaks centered at 420nm (violet emission), 450nm (violet-blue) and broad peak covering from 480 to 700nm (green, yellow, orange and red emissions). For ZnO nanoflowers LEDs, the emission peaks centered at 400nm (violet emission), 450nm (violet-blue) and a broad peak covering EL emissions from 480 to 700nm (green, yellow, orange and red emissions) were detected. ZnO nanorods and nanotubes LEDs showed the same EL spectra, and EL peaks centered at 400nm (violet emission), 450nm (violet-blue) and 540nm (green emission) were observed. For ZnO nanostructures (nanowalls, nanorods, nanoflowers and nanotubes)/p-GaN LEDs, the color rendering indices (CRI) were 95, 93, 87 and 88, and the correlated color temperatures were 6518, 5471, 4807 and 4801K, respectively.

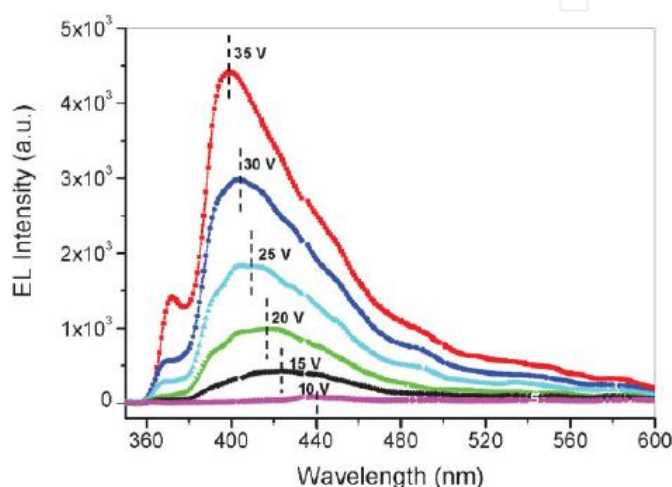


Figure 9. The electroluminescence spectrum of the (n-ZnO NWs)/(p-GaN film) LED device under various forward bias voltages (10, 15, 20, 25, 30, 35V), showing broad emission peaks from UV to blue and blue shift with increasing of bias voltage. From Ref. [69].

Xi et al fabricated heterojunction NiO/ZnO LEDs using low temperature solution-based growth method [77]. The devices exhibited room-temperature electroluminescence, and the steady increase of the UV-to-visible emission ratio was obtained for increased bias voltage, which was good agreement with some of the reported behavior of ZnO LEDs.

Klason et al reported the EL spectra obtained from ZnO nanodots/p-Si heterojunction LEDs [71]. The asymmetric EL emission peaked at around 600nm was observed and the emission from the devices having buffer layer were a bit blue shifted when compared to samples without the buffer layer. The buffer layer increased both the stability and efficiency of the devices.

Bano et al reported the ZnO-organic hybrid white LEDs grown on flexible plastic using low temperature aqueous chemical method [65]. Figure 10 shows the structure of ZnO-organic hybrid white LEDs, schematically. I-V curve of the device exhibited the typical rectifying behaviors. The EL spectrum displayed a broad emission band covering the whole visible region and hence provided white light. The white light emission was the superposition of a violet line (448nm), blue line (469nm) from the PFO combined with green emissions (503 and 541nm), and a red emission (620nm) due to deep level defect emissions in ZnO nano-

rods (Figure11). The color rendering index and correlated color temperature of the white LEDs were calculated to be 68 and 5800K, respectively (Figure12).

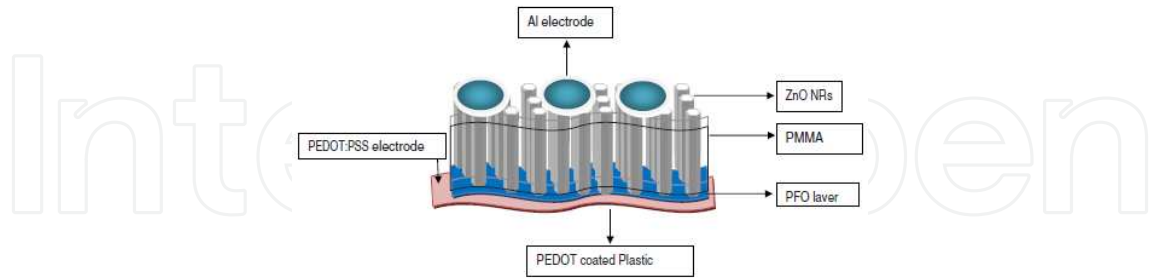


Figure 10. Schematic illustration of ZnO NRs/PFO hybrid device on PEDOT:PSS coated flexible plastic. From Ref. [65].

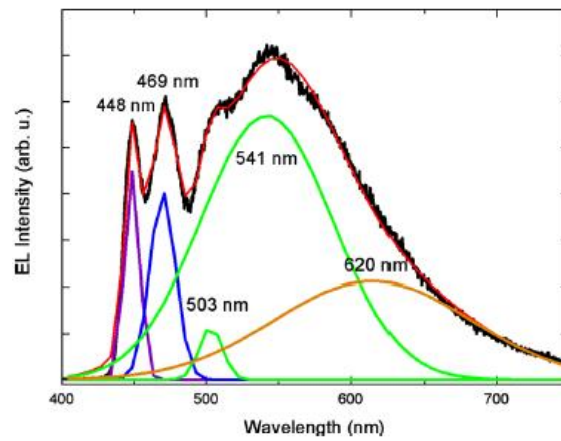


Figure 11. Room temperature EL spectrum and Gaussian fitting of the PFO/ZnO hybrid white LED. Inset: a photograph of white light emission from flexible device folded at a large angle during operation. From Ref. [65].

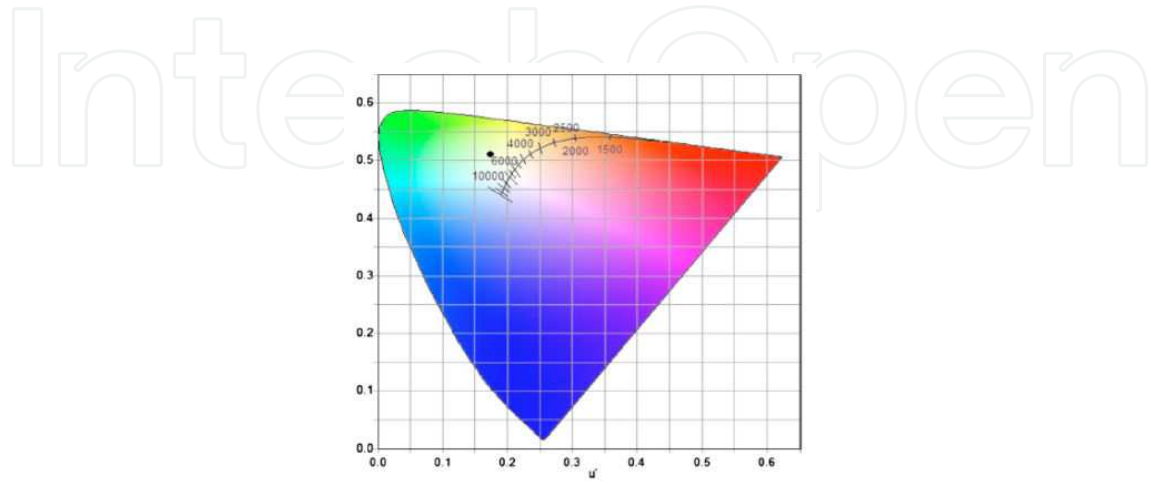


Figure 12. Typical color coordinates characteristics of the ZnO – PFO hybrid white LEDs. From Ref. [65].

4.1.3. *p*-ZnO heterojunction LEDs

Currently, the fabrication of *p*-type ZnO materials has made remarkable progress and some researchers attempted to prepare *p*-type ZnO based heterojunction LEDs by various methods, as summarized in Table 3.

Growth technique	Structure	Light emission (nm)	Reference
MBE	p-ZnO:Sb/i-ZnO/n-Si	381, 485, 612, 671	[79]
	p-ZnO:Sb/CdZnO/n-Si	459, 392	[80]
	p-MgZnO:N/n-ZnO bulk	382	[81]
MOCVD	p-ZnO:Sb/InGaNMQW/n-GaN	468	[82]
	p-ZnO:N/n-GaN:Si	390	[83]
Magnetron sputtering	p-ZnO:P/n-GaN	409	[84]
	p-ZnO:As/n-GaN film	382, 601, 647	[85]
	p-ZnO:P/n-Si	550	[86]
PLD	p-ZnO:P/Zn _{0.9} Mg _{0.1} O/ZnO/Zn _{0.9} Mg _{0.1} O/n-ZnO:Ga	385	[87]
Solution method	p-ZnO:K/n-GaN	372, yellow-orange	[88]

Table 3. Structure and emission of *p*-type ZnO based heterojunction LEDs

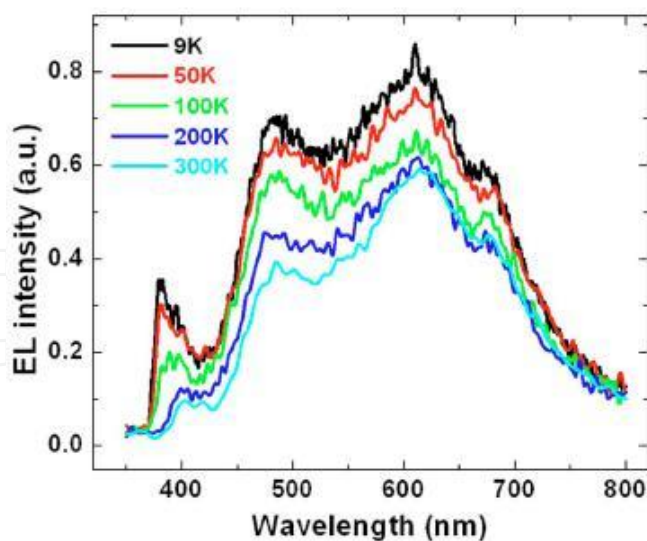


Figure 13. Temperature dependent EL spectra obtained at an injection current of 110 mA. EL from LED is obtained at 9, 50, 100, 200, and 300 K. From Ref. [79].

Mandalapu et al reported ultraviolet emission from Sb-doped *p*-type ZnO based heterojunction LEDs fabricated by growing *p*-type ZnO:Sb films on *n*-type Si substrates [79]. Thin un-

doped ZnO film(50nm) was grown at low temperature on *n*-Si(100) substrate as a buffer layer, followed by *p*-type ZnO:Sb layer (370nm) at a higher temperature by MBE. After the growth, thermal activation of Sb dopant was carried out in *in situ* in vacuum at 800°C for 30 min. The I-V curves of the heterojunction LEDs displayed a typical rectifying behavior with higher leakage current at both higher temperatures and higher biases, which may origin from the band alignment of wide-band-gap *p*-ZnO and narrow-band-gap *n*-Si. Figure13 shows the EL spectra obtained at different temperatures for an injection current of 110mA. Four emission peaks at 381, 485, 612 and 671nm were detected from the spectra at 9 K. The peak at 381nm was the near-band edge emission and the other peaks were attributed to intrinsic defects in ZnO. A small UV peak at 396nm was also observed in the EL spectra at 9K, which was related to Zn vacancies. With increasing temperature in the range from 9 to 300K, both the small UV peak and the near band edge emission redshifted and became a single peak at higher temperatures. The intensity of emissions decreased throughout the spectra with increasing temperature, which was due to the increase in nonradiative recombinations at higher temperatures.

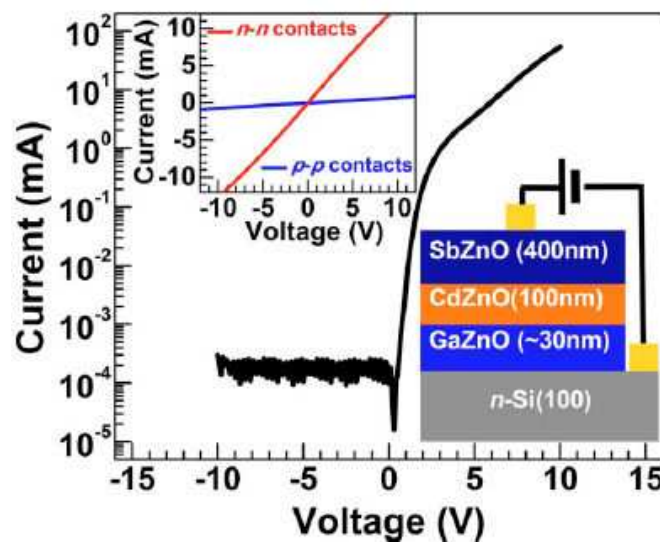


Figure 14. I-V curve of the device, showing rectifying characteristics. Top inset shows the linear I-V of *n*-contacts (red line) and *p*-contacts (blue line), respectively. Bottom inset shows device structure of the sample: SbZnO/CdZnO/GaZnO/Si. From Ref. [80].

Li et al reported on the blue electroluminescence from ZnO based heterojunction LEDs with CdZnO active layers [80]. *p*-ZnO:Sb/*i*-CdZnO/*n*-ZnO was grown on *n*-type Si substrates by plasma-assisted molecular-beam epitaxy. Figure14 shows the typical rectifying characteristics of the heterojunction LEDs, and the top inset of Figure14 reveals the I-V curves of Au/Ni and Au/Ti metal contacts on *p*-type ZnO:Sb and *n*-type Si, respectively, indicating that good ohmic contacts were formed on both electrodes. The PL spectra showed ZnO near band edge (NBE) emission of *p*-type ZnO:Sb at 378nm and NBE emission of CdZnO active layer at 445nm. Figure15 shows EL spectra of a hereojunction under different injection currents. The blue EL emissions at around 459nm were observed and the emission intensity increased

with the increase of the injection current. A comparison of PL and EL spectra of the device shows that the EL emission of the device originated from the radiative recombinations in CdZnO active layers in the film.

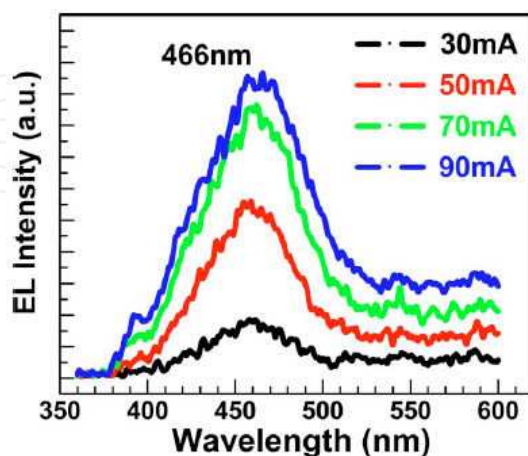


Figure 15. Room temperature EL characteristics of the LEDs under different injection currents. From Ref. [80].

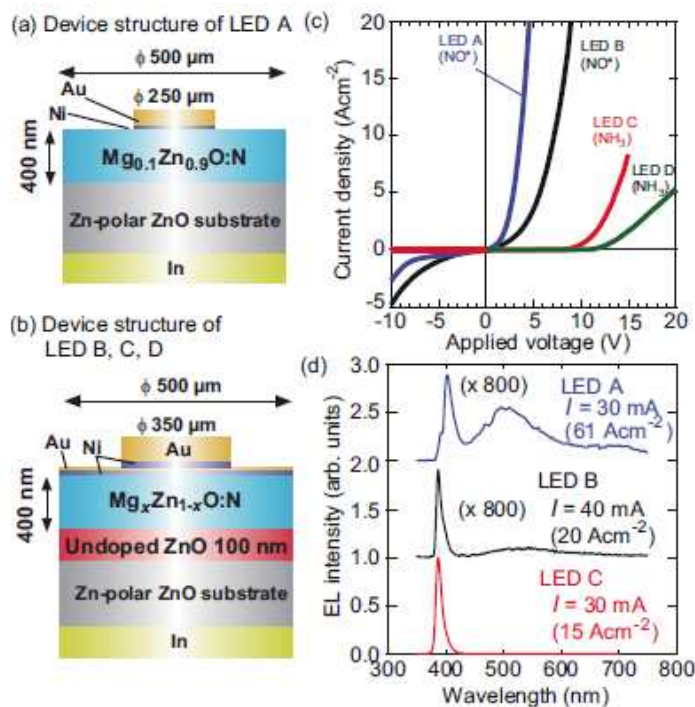


Figure 16. a) and (b) depict cross-sectional schematics for LED A and those of B–D, respectively. The device was 500 μm in diameter and the back side of the ZnO substrates was bonded to a metal plate with In. The top electrode in (a) was formed as Au(200 nm)/Ni(10 nm) with a diameter of 250 μm . That of (b) consists of a semitransparent electrode of Au (4 nm)/Ni (2 nm) with a diameter of 500 μm and a contact pad of Au (500 nm)/Ni (2 nm) with a diameter of 350 μm . (c) The rectifying I - V curve measured for LEDs A, B, C, and D. (d) EL spectra from LEDs A–C. All spectra were measured at room temperature. Forward bias operation conditions are also shown. From Ref. [81].

Nakahara et al fabricated heterostructure LEDs by growing N-doped p-type $Mg_xZn_{1-x}O$ layer by MBE on Zn face ZnO crystal using NO and NH_3 as N source [81]. The structures of the LEDs were shown in Figures 16(a) and (b). The I-V curves of the LEDs exhibited a rectifying property [Figure 16(c)]. LEDs A and B (NO as N source) had a turn-on voltage of approximately 3V, LEDs C and D (NH_3 as N source) showed a turn-on voltage of 10V. In the EL spectra of LEDs A and B, a sharp EL peak at the near band edge ($\lambda = 380 - 400\text{nm}$) was seen, indicating an effective blocking of electrons by the wide band gap $Mg_{0.1}Zn_{0.9}O:N$ layers and efficient exciton recombination in the n-type ZnO layers [Figure 16(d)]. The EL of LED C was much more intense by a factor of 800 than those of LEDs A and B.

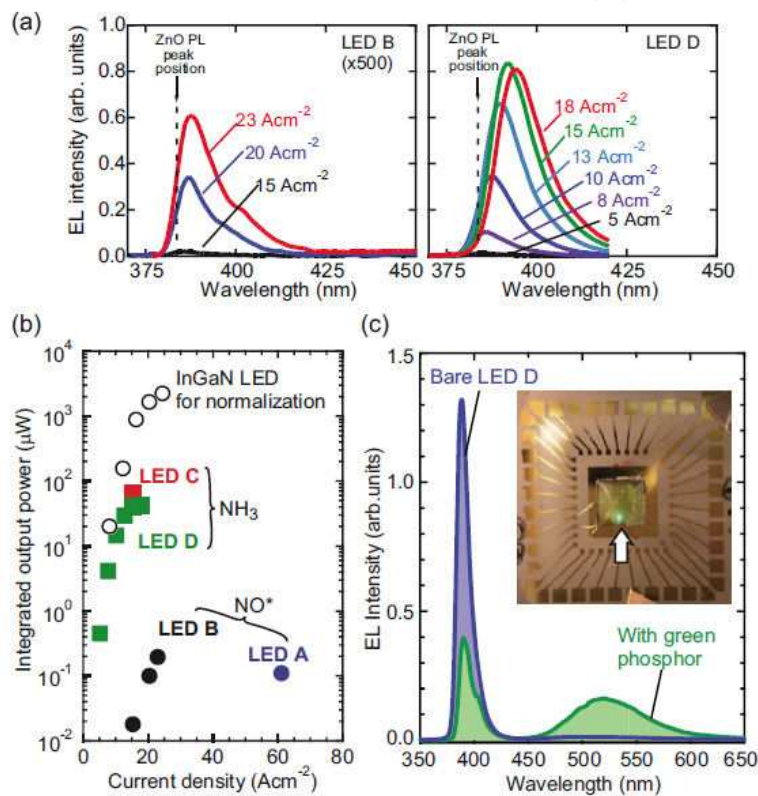


Figure 17. a) EL spectra of the LEDs B and D operated with various current densities. (b) Integrated EL intensity for the spectra shown in (a) (LEDs B and D) as a function of applied current density. The data for LEDs A and C are also shown. The integration was conducted in a wavelength range from 350 to 450 nm. (c) EL spectra for bare and with a green phosphor coating for LED D at an operation current of 40 mA. Inset is a picture taken under standard laboratory illumination. Emission from the phosphor can be clearly seen as indicated by an arrow. From Ref. [81].

The EL peak energies of the LEDs were slightly lower than the PL peak energy of ZnO, which were due to the self-absorption of the ZnO emission in the thick ZnO substrate and the heating effect during the operation [Figure 17(a)]. The outpower of the LEDs ranged from 0.1 to $70\mu\text{W}$ at the maximum attainable operation current (typically 30–40mA)[Figure 17(b)]. Interestingly, when LED was coated with a 0.1-mm-thick epoxy resin containing 5wt % $(BaEu)(MgMn)Al_{10}O_{17}$ green phosphor, a part of ultraviolet NBE in the EL spectrum of the LED was converted into green, indicating that the UV emission may excite many existing phosphors developed for fluorescent tube and enable better color rendering [Figure 17(c)].

Growth technique	Structure	Light emission (nm)	Reference
MBE	p-ZnO:N/i-ZnO/n-ZnO	Violet-green	[5]
	p-ZnO:N/n-ZnO	420	[89]
	p-ZnO:Sb/n-ZnO:Ga	383.3, 490, 605	[90]
	p-ZnO:Sb/n-ZnO:Ga	385-393	[91]
MOCVD	p-ZnO:N/n-ZnO/ZnO bulk	372, 435, 520	[92]
	n-ZnO/p-ZnO:As/GaAs	388, 496	[93]
	n-ZnO:Ga/p-ZnO:N	388, 516	[94]
Ion implantation	p-ZnO:N/n-ZnO bulk	530, 740	[95]
	p-ZnO:As nanorod /n-ZnO nanorod	380, 630	[96]
	p-ZnO:P nanorod /n-ZnO nanorod	UV, 510, 800	[97]
Magnetron sputtering	p-ZnO:P /n-ZnO	380, 640	[98]
Solution method	p-ZnO:P nanorod / n-ZnO film	415, 450-650	[99]
Hybrid beam deposition	p-ZnO:As /p-Be _{0.3} Zn _{0.7} O / (ZnO/Be _{0.2} Zn _{0.8} O)MQW/ n-Be _{0.3} Zn _{0.7} O/n-ZnO	363, 388, 550,	[100]

Table 4. Structure and emission of ZnO based homojunction LEDs.

Park et al reported on the growth and device properties of *p*-ZnO/(InGaN/GaN) multi-quantum well (MQW)/*n*-GaN heterojunction LEDs [82]. A GaN buffer layer (30nm) was deposited on a sapphire substrate. After high temperature annealing of the buffer layer, undoped GaN(5μm), *n*-type GaN:Si(2μm) and InGaN/GaN MQW were grown by MOCVD, then, *p*-type ZnO:Sb layer was deposited on InGaN/GaN MQW. Finally, to active *p*-type dopant, a rapid thermal annealing was performed in an N₂ ambient for 1min. The emission peak at 468nm was observed at room temperature, and the emission intensity of the LEDs increased as injection current increased, indicating that *p*-ZnO:Sb layer acted as a hole supplying layer in the hybrid LEDs. The emission peak red shifted as injection current increased due to the decrease in strain-induced piezoelectric field in the InGaN well by Sb-doped *p*-ZnO and Joule heating. Similarly, Hwang et al prepared *p*-ZnO:P/*n*-GaN heterostructure LEDs [84]. The PL spectra of the *p*-ZnO and *n*-GaN films exhibited the emission peaks at 365nm and 385nm, corresponding to NBE emissions of *n*-type GaN and *p*-type ZnO, respectively. Under forward bias, an EL emission at 409nm at room temperature were observed, which was attributed to the band gap of *p*-ZnO:P grown on *n*-GaN.

4.1.4. Homojunction LEDs

Based on the fabrication of p-type ZnO materials, some researchers reported on ZnO-homojunction LEDs. Table 4 is a survey of structure, method and emission peak of ZnO-homojunction LEDs.

Tsukaza et al fabricated ZnO p-i-n homojunction LEDs by laser MBE using N as acceptor dopant [5]. The structure of the device was shown in Figure 1(a). To realize an automatically flat interface, the homojunction structure was grown in layer-by layer. The I-V curve of the LED exhibited a rectifying behavior with a threshold voltage of 7V [Figure 1(b)]. The threshold voltage was higher than the bandgap of ZnO (3.3eV), which was mainly attributed to the high resistivity of the p-type ZnO layer. The EL spectrum of the homojunction LED showed luminescence from violet to green regions with multi-reflection interference fringes. Compared PL spectrum of p-type ZnO and EL spectrum obtained from the LED, the higher energy side peak around 430nm in the EL spectrum matches well with the PL spectrum [Figure 1(c)].

Chu et al reported on homojunction UV LEDs based on p-type Sb-doped ZnO/n-type Ga-doped ZnO films. ZnO homojunction was grown on n-type Si(100) substrates by MBE [90]. A thin MgO/ZnO buffer layer was deposited to reduce the lattice mismatch between Si and ZnO, then, the two layer structured Sb-doped p-type ZnO (420nm)/Ga-doped n-type ZnO (420nm) homojunction was grown on this MgO/ZnO buffer. After the growth, *in situ* thermal annealing was performed to active Sb dopant in ZnO:Sb films. The I-V curve p-ZnO:Sb/n-ZnO:Ga homojunction exhibited rectifying characteristics with a threshold voltage of 6V. Figure 18 shows room temperature EL of the homojunction LEDs under different injection currents. The NBE emission at ~383 nm was observed, the other peaks around 490 and 605nm related to intrinsic defects were also detected. With the increase of the injection current, the NBE emission redshifted from 383.3nm (30mA) to 390.9nm (100mA), which was induced by the band gap variations due to the increased heating effects during the operation of LEDs.

Similarly, Kong et al fabricated Sb-doped p-type ZnO/Ga-doped n-type ZnO homojunction on Si (100) substrate [91]. I-V and C-V curves presented typical electrical properties of a diode. The EL emission of the homojunction LEDs demonstrated dominant UV emissions. A NBE emission at 3.2eV started to appear when the current is 60mA. When the injection current increases from 60 to 100mA. The intensity of the UV emission increased and the emission peak slightly redshifted from 385 to 393nm. The output power of this LED was estimated to be only 1nW at drive current of 100mA.

Wei et al prepared ZnO homojunction LEDs on c-plane Al₂O₃ substrates by plasma-assisted MBE using a gas mixture of N₂ and O₂ as the p-type dopant [89]. At low temperature (100K), the I-V curve of the LEDs exhibited a typical rectifying behavior with a threshold voltage of 4.0V at forward bias and a low leak current at reversed bias voltage. The LED keeps a good rectifying characteristic even as increasing temperature up to 300K. A emission at 2.83eV started to appear when the current was 2.42mA. The emission peak blue shifted from 2.83 to 2.95eV as the injection current changed from 2.42 to 3.31mA, indicating that the EL emission

originated from the donor-acceptor pair recombination in the p -type ZnO layer. The LED can even emit intensive EL in the blue-violet region at the temperature of 350K.

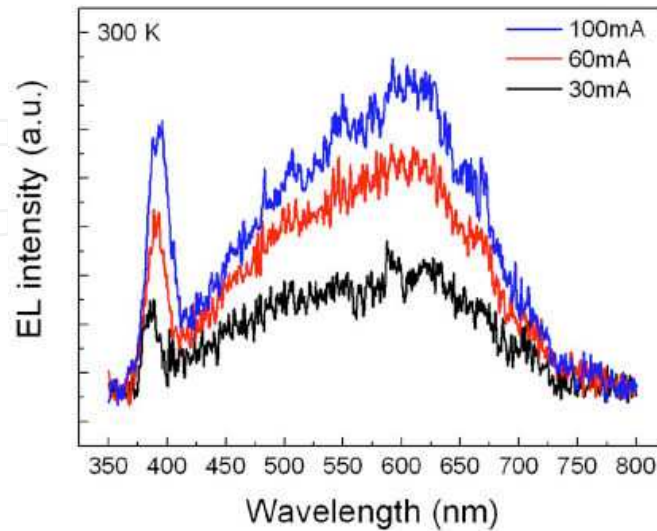


Figure 18. Room temperature EL spectra at different injection current from 30 to 100mA. From Ref.[90].

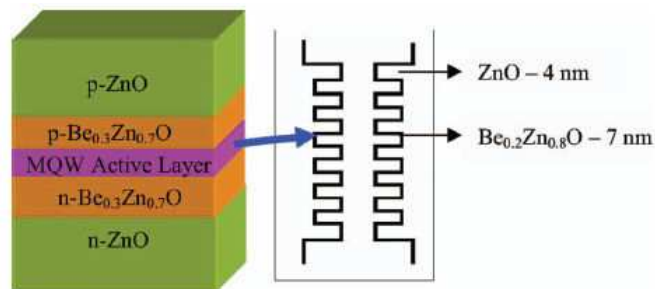


Figure 19. Schematic illustration of the structure of the ZnO-based UV LED devices that employ a BeZnO/ZnO active layer comprised of MQWs. From Ref. [100].

Sun et al reported on the ultraviolet electroluminescence from ZnO homojunction with n -ZnO/ p -ZnO:As/GaAs structure [93]. To obtain p -type ZnO film, firstly, a 400nm ZnO layer was deposited on p -GaAs (100) substrate at 450°C by MOCVD, followed by a thermal annealing at 550°C in 20Pa oxygen ambient for 30min to enhance the diffusion of arsenic and activate the acceptor impurities. After the thermal annealing, a 300nm undoped n -type ZnO layer was grown on the ZnO:As film at 350°C. The ZnO homojunction had a rectifying behavior with a turn-on voltage of about 4V and a reverse breakdown voltage of higher than 6V. Under forward injection current of 30mA, the EL emission exhibited two independent bands centered at 3.2 and 2.5eV, which could be assigned to the NBE emission and deep-level emission, respectively.

Ryu et al reported on ZnO-based UV LEDs fabricated by the hybrid beam deposition [100]. The LEDs employed a BeZnO/ZnO active layer between *n*-type and *p*-type ZnO and Be_{0.3}Zn_{0.7}O layers, as shown in Figure19. The active layer is composed of seven quantum wells for which undoped Be_{0.2}Zn_{0.8}O (7nm) and ZnO (4nm) form barrier and well layers, respectively. The *p*-type ZnO and BeZnO layers were prepared with As as the acceptor dopant and *n*-type ZnO and BeZnO layers were formed with Ga as the dopant. The I-V curve of the LEDs exhibited a typical rectifying behavior with a high threshold voltage and a low reverse bias current.

Figure20 shows the EL spectra of the LEDs at room temperature. The peaks centered 388nm (bound exciton — BE) and 550nm (green band — GB) were the dominant features at low forward currents (≤ 20 mA), which were attributed the impurity (donor or acceptor)-bound exciton emission and donor-acceptor pair recombination. As the current injection levels was above 20mA, the peak at 363nm becomes the prominent spectral feature and the peaks at 388 and 550nm have become saturated. The peak at 363nm could be assigned to band-to-band recombination, such as from localized-exciton peaks in the active layer of the QWs.

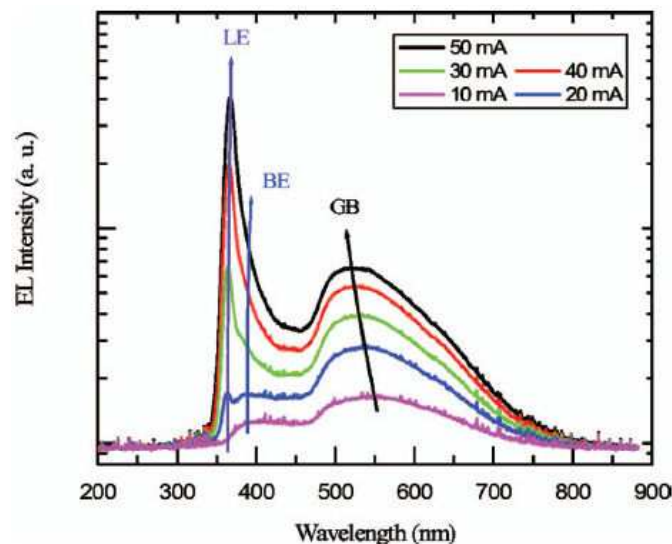


Figure 20. EL spectrum measured at room temperature in continuous current mode of a *p-n* junction ZnO-based LED having a BeZnO active layer. The primary spectral emission peak is located near 363 nm and arises from localized-exciton emissions in the QWs. The secondary peak centered near 388 nm is from impurity-bound exciton emissions in ZnO. From Ref. [100].

Lim et al fabricated UV LEDs based on ZnO *p-n* homojunction [98]. A Ga-doped ZnO layer (1.5 μ m) were grown on a *c*-Al₂O₃ substrates at 900°C by sputtering a ZnO target mixed with 1 wt% Ga₂O₃. A *p*-type ZnO layer (0.4 μ m) was grown in situ on the *n*-type ZnO layer at 900°C by sputtering a ZnO target mixed with 1 wt% P₂O₅. A rapid thermal annealing process was performed to the LEDs for 5min at 800°C in a nitrogen atmosphere in order to activate the *p*-type ZnO layers. The I-V curve of the device showed clear rectification with a threshold voltage of 3.2V, which was good agreement with the ZnO bandgap energy (3.37eV). The EL spectra of the ZnO homojunction LED is shown in Figure21. A NBE emission at 380nm and broad deep-level emissions at approximately 640nm were observed. The

EL spectra of the LED matched well with the PL spectrum of the p-type ZnO film, indicating that the recombination of electrons and holes occurred mostly in p-type ZnO layer.

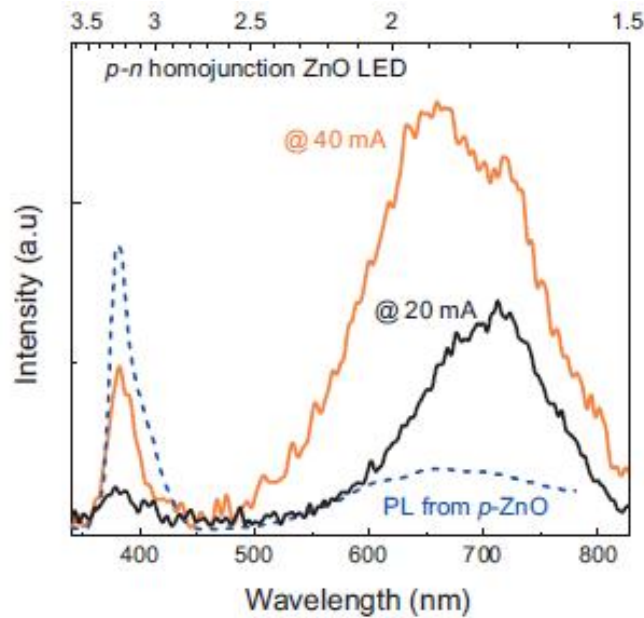


Figure 21. EL spectra of p-n homojunction ZnO LED operated at forward currents of 20 and 40 mA; PL spectrum of p-type ZnO obtained at room temperature. From Ref. [98].

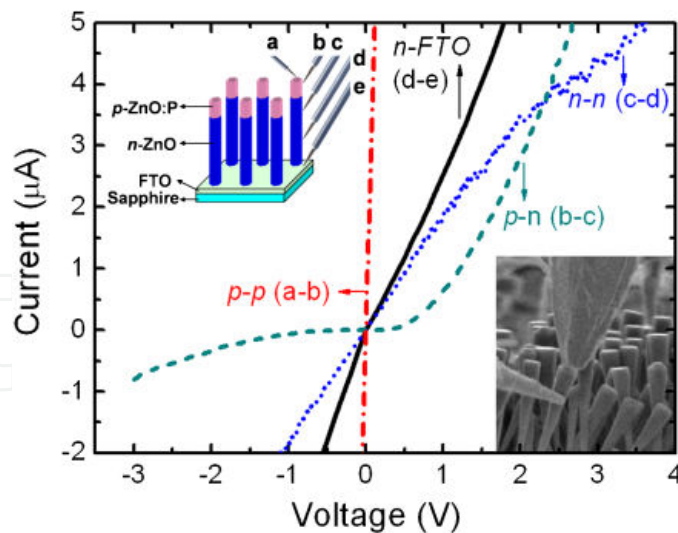


Figure 22. I-V characteristics of p-p, p-n, n-n, and n-FTO regions in a single ZnO rod. The upper left and lower right insets show the schematic diagram and a SEM image of probing by Zyex nanomanipulator, respectively. From Ref. [97].

Sun et al reported on UV emission from a ZnO rod homojunction LED [97]. Vertically aligned ZnO rods (Diameters: 200–500nm; Length:3.5 μ m) were uniformly grown on fluo-

rine-doped tin oxide (FTO) coated sapphire *c*-plane substrates by a vapor phase transport method. After the growth, ZnO rod arrays were implanted with P⁺ ions with 50keV (device I) and 100keV (device II) at a dosage of $1 \times 10^{14} \text{ cm}^{-2}$ perpendicular to the aligned rods. The implanted ZnO rods were annealed at 900°C for 1 h with an O₂ flow rate of 100 SCCM at 1Torr to active p-type dopant. Figure 22 exhibits the typical *I-V* characteristics of different regions in a single vertically aligned *p*-ZnO:P/*n*-ZnO rod. The rectifying behavior with a threshold voltage of 0.8V was observed for *p-n* junction. The near-linear relationship was also detected for *p-p*, *n-n*, and *n*-FTO curves, indicating an Ohmic behavior.

Figure 24 displays the EL spectra of ZnO rod homojunction LEDs at various injection currents. Strong UV emission was observed from both devices, corresponding to the NBE emission of ZnO. The UV light output intensities increased linearly as injection current was above a threshold current (Figure 23 insets). In addition, device I shows a relatively weak and broad emission band in the visible range, indicating a low density of deep-level defects, and the broad emission consisted of one green emission (~510nm) and one nearinfrared peak (~800nm) became stronger for device II. Similarly, Yang et al fabricated ZnO nanorod *p-n* homojunction LEDs with As implantation [96]. The EL spectrum of the device exhibited a strong UV band centered at ~380 nm and a weak broad red band peaking at ~630nm.

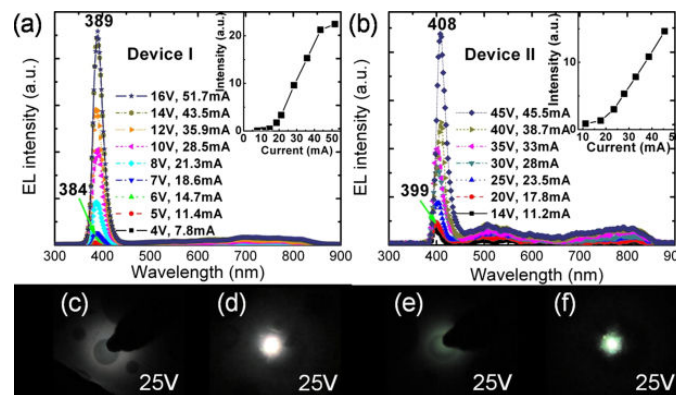


Figure 23. EL spectra of (a) device I and (b) device II under various injection currents, respectively. The insets show the UV light output intensities as a function of forward injection current. The photographs of corresponding light emissions collected from both (c) and (e) front side (Au anode) and (d) and (f) back side single-sided polished sapphire substrate in these two devices under the same bias voltage of 25 V. From Ref. [97].

5. Conclusion and outlook

With a large direct band gap of 3.37eV and a large exciton binding energy of 60meV, ZnO has attracted much attention for its application in optoelectronics applications, such as LEDs, photodetector and laser diodes. In the paper, based on the introduction of the band-gap engineering and doping in ZnO, we presented a comprehensive review of ZnO-based LEDs. Band-gap engineering in ZnO can be achieved by alloying with MgO, CdO or BeO. Theoretically, the energy band gap of $A_xZn_{1-x}O$ can be continuously modulated from 0.9eV

(CdO) to 10.6eV (BeO) by changing the A concentration. As a n-type semiconductor, high quality n-type ZnO materials can be obtained by doping doping III elements (Al, Ga and In). Although the fabrication of p-type ZnO remain great challenges due to the self-compensation, p-type ZnO have been prepared by doping different elements (N, P, As, Sb, Li, Na and K) with various techniques. ZnO based heterojunction and homojunction LEDs have been achieved, which makes ZnO as a strong candidates for solid-state light. Although the efficiency of ZnO-based LEDs is not high, improvements are rapid and the emitters have the potential to outperform their GaN rivals.

ZnO-based LEDs show great promise for the future, however, there are some severe issues that are in need of further investigation to transition ZnO-based LEDs to commercial use from the current stage. One problem is that the usable, reproducible p-type ZnO are not easy to fabricate, although some researchers have been successful. Another is the achievement of high quality p-n junction based ZnO. The p-n junction with good threshold and breakdown voltages is necessary for the LEDs. In addition, diode-like behavior and light emission have been observed, however, the mechanism of the properties remain unclear.

6. Acknowledgements

The work was supported by the Fundamental Research Funds for the Central Universities (Contract No: 531107040334) and the Aid Program for exploring investigation (Contract No: 513280501).

Author details

J.C. Fan¹, S.L. Chang² and Z. Xie¹

1 College of Physics and Microelectronics Science, Key Laboratory for Micro-Nano Physics and Technology of Hunan Province, Hunan University, Changsha 410082, People's Republic of China

2 Center of Materials Science, College of Science, National University of Defense Technology, Changsha, 410073, People's Republic of China

References

- [1] Choi Y-S, Kang J-W, Hwang D-K , Park S-J. Recent advances in ZnO-based light-emitting diodes, *IEEE Trans. Electr. Dev.* 2010; 57,26-41.
- [2] Janotti A, Van de Walle CG. Fundamentals of zinc oxide as a semiconductor, *Rep. Prog. Phys.* 2009; 72, 126501 (29pages).

- [3] Özgür Ü, Alivov C, Liu C, Teke A, Reshchikov A, Doğan S, Avrutin V, Cho S-J, Morkoç H. A comprehensive review of ZnO materials and devices, *J. Appl. Phys.* 2005; 98, 041301(103pages).
- [4] Look D.C. , Recent advances in ZnO materials and devices, *Mater. Sci. and Eng. B* 2001; 80, 383-387.
- [5] Tsukazaki A, Ohtomo A, Onuma T, Ohtani M, Makino T, Sumiya M, Ohtani K, Chichibu SF, Segawa Y, Ohno H, Koinuma H, Kawasaki M. Repeated temperature modulation epitaxy for p-type doping and light-emitting diode based on ZnO. *Nat. Mater.* 2005; 4, 42-46.
- [6] Chen SC, Chen MJ, Huang YH, Sun W C, Li W C, Yang J R, Kuan H, Shiojiri M. White-light electroluminescence from n-ZnO/p-GaN heterojunction light-emitting diodes at reverse breakdown bias. *IEEE Trans. Electron Devices* 2011; 58, 3970-3975.
- [7] <http://optics.org/article/26093>
- [8] Ryu YR, Lee TS, Lubguban J A, Corman A B, White H W, Leem J H, Han M S, Park YS, Youn C J, Kim WJ. Wide-band gap oxide alloy: BeZnO. *Appl. Phys. Lett.* 88, 052103(3pages).
- [9] Han MS, Kima JH, Jeonga TS, Parka JM, Youn CJ, Leem JH, Ryu YR. Growth and optical properties of epitaxial $\text{Be}_x\text{Zn}_{1-x}\text{O}$ alloy films. *J. Cryst. Growth* 2007; 303, 506-509.
- [10] Ohtomo A, Kawasaki M, Koida T, Masubuchi K, Koinuma H, Sakurai Y, Yoshida Y, Yasuda T, Segawa Y. $\text{Mg}_x\text{Zn}_{1-x}\text{O}$ as a II-VI wide-gap semiconductor alloy. *Appl. Phys. Lett.* 1998; 72, 2466-2468 (3pages).
- [11] Takagi T, Tanaka H, Fujita S, Fujita S. Molecular beam epitaxy of high magnesium content single-phase wurtzite $\text{Mg}_x\text{Zn}_{1-x}\text{O}$ alloys (x similar or equal to 0.5) and their application to solar-blind region photodetectors. *Jpn. J. Appl. Phys.* 2003; 42, L401-L403.
- [12] Tampo H, Shibata H, Maejima K, Yamada A, Matsubara K, Fons P, Niki S, Tainaka T, Chiba Y, Kanie H. Strong excitonic transition of $\text{Zn}_{1-x}\text{Mg}_x\text{O}$ alloy. *Appl. Phys. Lett.* 91, 261907(3pages).
- [13] Wassner T A, Laumer B, Maier S, Laufer A, Meyer B K, Stutzmann M, Eickhoff M. (2009), Optical properties and structural characteristics of ZnMgO grown by plasma assisted molecular beam epitaxy. *J. Appl. Phys.* 2009; 105, 023505 (6pages).
- [14] Makino T, Segawa Y, Kawasaki M, Ohtomo A, Shiroki R, Tamura K, Yasuda T, Koinuma H. Band gap engineering based on $\text{Mg}_x\text{Zn}_{1-x}\text{O}$ and $\text{Cd}_y\text{Zn}_{1-y}\text{O}$ ternary alloy films. *Appl. Phys. Lett.* 2001; 78, 1237-1239.
- [15] Lai H H-C, Kuznetsov V, Egdell RG, Edwards PP. Electronic structure of ternary $\text{Cd}_x\text{Zn}_{1-x}\text{O}$ ($0 \leq x \leq 0.075$) alloy. *Appl. Phys. Lett.* 100, 072106 (4 pages).
- [16] Chauveau J-M, Teisseire M, Kim-Chauveau H, Morhain C, Deparis O, Vinter B. Anisotropic strain effects on the photoluminescence emission from heteroepitaxial and ho-

- moepitaxial nonpolar (Zn,Mg)O/ZnO quantum wells. *J.Appl.Phys.*109,102420 (6pages).
- [17] Su SC, Lu Y M, Zhang Z Z, Shan C X, Yao B, Li B H, Shen D Z, Zhang J Y, Zhao D X, Fan XW. The optical properties of ZnO/ZnMgO single quantum well grown by P-MBE. *Appl. Surf. Sci.*2008; 254, 7303–7305.
- [18] Kim K-K, Niki S, Oh J-Y, Song J-O, Seong T-Y, Park S-J, Fujita SZ, Kim S-W. High electron concentration and mobility in Al-doped n-ZnO epilayer achieved via dopant activation using rapid-thermal annealing. *J.Appl.Phys.*97,066103 (6pages).
- [19] Kim Y M, Lee W J, Jung D-R, Kim J M, Nam SH, Kim H C, Park BW. Optical and electronic properties of post-annealed ZnO:Al thin films. *Appl. Phys. Lett.* 2010; 96, 171902 (3pages).
- [20] Bhosle V, Tiwari A, Narayan J. Electrical properties of transparent and conducting Ga doped ZnO. *J. Appl. Phys.*2006; 100, 033713 (6pages).
- [21] Yamada T, Miyake A, Kishimoto S, Makino H, Yamamoto N, Yamamoto T. Low resistivity Ga-doped ZnO thin films of less than 100 nm thickness prepared by ion plating with direct current arc discharge. *Appl. Phys. Lett.* 2007;91,051915(3pages).
- [22] Liang S, Bi X F. Structure, conductivity, and transparency of Ga-doped ZnO thin films arising from thickness contributions. *J.Appl.Phys.*2008;104,113533 (5pages).
- [23] Wang B G, Callahan MJ, Xu CC, Bouthillette LO, Giles NC, Bliss DF. Hydrothermal growth and characterization of indium-doped-conducting ZnO crystal. *J. Cryst. Growth.*2007; 304, 73-79.
- [24] Quang LH, Kuan LS, Liang GGK. Structural and electrical properties of single crystal indium doped ZnO films synthesized by low temperature solution method. *J.Cryst.Growth*2010; 312, 437-442.
- [25] Chen KJ, Hung FY, Chang SJ, Hu ZS. Microstructures, optical and electrical properties of In-doped ZnO thin films prepared by sol-gel method. *Appl. Surf. Sci.*2009; 255, 6308-6312.
- [26] Cao L, Zhu LP, Jiang J, Zhao R, Ye ZZ, Zhao BH. Highly transparent and conducting fluorine-doped ZnO thin films prepared by pulsed laser deposition. *Sol. Energ. Mat.Sol. C.*2011; 95, 894-898.
- [27] Chikoidze E, Modreanu M, Sallet V, Gorochovo O, Galtier P. (2008), Electrical properties of chlorine-doped ZnO thin films grown by MOCVD, *Phys. Stat. Sol. (A)*2008; 205, 1575–1579.
- [28] Liu W W, Yao B, Zhang ZZ, Li WF, Li BH, Shan CX, Zhang J Y, Shen D Z, Fan XW. Doping efficiency, optical and electrical properties of nitrogen-doped ZnO films. *J. App. Phys.*2011; 109,093518 (5pages).
- [29] Zeng YJ, Ye ZZ, Xu WZ, Liu B, Che Y, Zhu LP, Zhao BH. Study on the Hall-effect and photoluminescence of N-doped p-type ZnO thin films. *Mater.Lett.*2007; 61, 41-44.

- [30] Wang C, Ji ZG, Xi JH, Du J, Ye Z Z. Fabrication and characteristics of the low-resistive p-type ZnO thin films by DC reactive magnetron sputtering. *Mater. Lett.* 2006; 60, 912-914.
- [31] Kumar M, Kim T-H, Kim S-S, Lee B-T. Growth of epitaxial p-type ZnO thin films by codoping of Ga and N. *Appl. Phys. Lett.* 2006; 89, 112103 (3 pages).
- [32] Park CH, Zhang SB, Wei S-H. Origin of p-type doping difficulty in ZnO: The impurity perspective. *Phys. Rev. B* 2002; 66, 073202 (3 pages).
- [33] Limpijumnong S, Zhang S B, Wei S-H, Park CH. Doping by large-size-mismatched impurities: the microscopic origin of Arsenic or Antimony-doped p-type Zinc Oxide. *Phys. Rev. Lett.* 2004; 92, 15504 (4 pages).
- [34] Xiu FX, Yang Z, Mandalapu L J, Liu J L. Donor and acceptor competitions in phosphorus-doped ZnO. *Appl. Phys. Lett.* 2006; 88, 152116 (3 pages).
- [35] Kim K K, Kim H-S, Hwang DK, Lim J-H, Park S-J. Realization of p-type ZnO thin films via phosphorus doping and thermal activation of the dopant. *Appl. Phys. Lett.* 2003; 88, 152116 (3 pages).
- [36] Pan X H, Jiang J, Zeng Y J, He H P, Zhu L P, Ye Z Z, Zhao B H, Pan X Q. Electrical and optical properties of phosphorus-doped p-type ZnO films grown by metalorganic chemical vapor deposition. *J. Appl. Phys.* 2008; 103, 023708 (4 pages).
- [37] Vaithianathan V, Lee B-T, Kim S S. Pulsed-laser-deposited p-type ZnO films with phosphorus doping. *Appl. Phys. Lett.* 2005; 98, 043519 (3 pages).
- [38] Ryu Y R, Lee T S, Leem J H, White H W. Fabrication of homostructural ZnO p-n junctions and ohmic contacts to arsenic-doped p-type ZnO. *Appl. Phys. Lett.* 2003; 83, 4032-4034.
- [39] Vaithianathan V, Lee B-T, Kim S S. Preparation of As-doped p-type ZnO films using a Zn₃As₂/ZnO target with pulsed laser deposition. *Appl. Phys. Lett.* 2005; 86, 062101 (3 pages).
- [40] Kang HS, Kim GH, Kim DL, Chang HW, Ahn BD, Lee SY. Investigation on the p-type formation mechanism of arsenic-doped p-type ZnO thin films. *Appl. Phys. Lett.* 2006; 89, 181103 (3 pages).
- [41] Guo W, Allenic A, Chen YB, Pan XQ, Che Y, Hu Z D, Liu B. Microstructure and properties of epitaxial antimony-doped p-type ZnO films fabricated by pulsed laser deposition. *Appl. Phys. Lett.* 2007; 90, 242108 (3 pages).
- [42] Xiu FX, Yang Z, Mandalapu L J, Zhao DT, Liu J L, Beyermann YP. High-mobility Sb-doped p-type ZnO by molecular-beam epitaxy. *Appl. Phys. Lett.* 2005; 87, 152101 (3 pages).
- [43] Yi JB, Lim CC, Xing GZ, Fan HM, Van LH, Huang SL, Yang KS, Huang XL, Wang BY, Wu T, Wang L, Zhang HT, Gao XY, Liu T, Wee ATS, Feng Y.P, Ding J. (2010), Ferromagnetism in dilute magnetic semiconductors through defect engineering: Li-doped ZnO. *Phys. Rev. Lett.* 2010; 104, 137201 (4 pages).

- [44] Lin SS, He HP, Lu YF, Ye ZZ. Mechanism of Na-doped p-type ZnO films: Suppressing Na interstitials by codoping with H and Na of appropriate concentrations. *J. Appl. Phys.* 2009; 106, 093508 (5 pages).
- [45] Wu J, Yang YT. Deposition of K-doped p type ZnO thin films on (0001) Al₂O₃ substrates. *Mater. Lett.* 2008; 62, 1899-1901.
- [46] Chang SP, Chuang RW, Chang SJ, Chiou YA, Lu CY. MBE n-ZnO/MOCVD p-GaN heterojunction light-emitting diode. *Thin Solid Films* 2009; 517, 5054-5056.
- [47] Wang SP, Shan CX, Zhu H, Li B H, Shen D Z, Liu XY, Tang Z K. Phosphor-converted light-emitting diode based on ZnO-based heterojunction. *J. Lumin.* 2010; 130, 2215-2217.
- [48] Zheng H, Mei ZX, Zeng Z Q, Liu Y Z, Guo LW, Jia JF, Xue Q K, Zhang Z, Du X L. Fabrication and characterization of high quality n-ZnO/p-GaN heterojunction light emitting diodes. *Thin solid films* 2011; 520, 445- 447.
- [49] Mares J W, Falanga M, Thompson AV, Osinsky A, Xie J Q, Hertog B, Dabiran A, Chow PP, Karpov S, Schoenfeld W V. Hybrid CdZnO/GaN quantum-well light emitting diodes. *J. Appl. Phys.* 2008; 104, 093107 (5 pages).
- [50] Osinsky A, Dong GW, Kauser MZ, Hertog B, Dabiran AM, Chow PP, Pearton SJ, Lopatiuk O, Chernyak L. MgZnO/AlGaN heterostructure light-emitting diodes. *Appl. Phys. Lett.* 2004; 85, 4272-4274.
- [51] Hwang S-H, Chung TH, Lee BT. Study on the interfacial layer in ZnO/GaN heterostructure light-emitting diode. *Mater. Sci. Eng. B* 2009; 157, 32-35.
- [52] Lee JY, Lee JH, Kim HS, Lee CH, Ahn H-S, Cho HK, Kim YY, Kong BH, Lee HS. A study on the origin of emission of the annealed n-ZnO/p-GaN heterostructure LED. *Thin Solid Films* 2009; 517, 5157-5160.
- [53] Han W S, Kim Y Y, Kong BH, Cho H K. Ultraviolet light emitting diode with n-ZnO:Ga/i-ZnO/p-GaN:Mg heterojunction. *Thin solid films* 2009; 517, 5106-5109.
- [54] Zhang SG, Zhang XW, Yin ZG, Wang JX, Dong JJ, Wang ZG, Qu S, Cui B, Wowchak AM, Dabiran AM, Chow P P. Improvement of electroluminescent performance of n-ZnO/AlN/p-GaN light-emitting diodes by optimizing the AlN barrier layer. *J. Appl. Phys.* 2011; 109, 093708 (6 pages).
- [55] Iwan S, Bambang S, Zhao JL., Tan ST, Fan HM, Sun L, Zhang S, Ryu HH, Sun XW. Green electroluminescence from an n-ZnO: Er/p-Si heterostructured light-emitting diode. *Physica B*, <http://dx.doi.org/10.1016/j.physb.2012.03.072> .
- [56] Ohta H, Kawamura K-I, Orita M, Hirano M, Sarukura N, Hosono H. Current injection emission from a transparent p-n junction composed of p-SrCu₂O₂/n-ZnO. *Appl. Phys. Lett.* 2000; 77, 475-477.

- [57] Rogers DJ, Teherani F H, Yasan A, Minder K, Kung P, Razeghi M. Electroluminescence at 375 nm from a ZnO/GaN:Mg/c-Al₂O₃ heterojunction light emitting diode. *Appl. Phys. Lett.* 2006; 88, 14198 (3 pages).
- [58] Yu QX, Xu B, Wu Q H, Liao Y, Wang GZ, Fang RC. Optical properties of ZnO/GaN heterostructure and its near-ultraviolet light-emitting diode. *Appl. Phys. Lett.* 2003; 83, 4713-4715.
- [59] Ye J D, Gu S L, Zhu S M, Liu W, Liu S M, Zhang R, Shi Y, Zheng Y D. Electroluminescent and transport mechanisms of n-ZnO/p-Si heterojunctions. *Appl. Phys. Lett.* 2006; 88, 182112 (3 pages).
- [60] Li XP, Zhang BL, Zhu HC, Dong X, Xia XC, Cui YG, Ma Y, Du GT. Study on the luminescence properties of n-ZnO/p-Si heterojunction diode grown by MOCVD. *J. Phys. D: Appl. Phys.* 2008; 41, 035101 (5 pages).
- [61] Alivov Y I, Kalinina E V, Cherenkov A E, Look D C, Ataev B M, Omaev A K, Chukichev M V, Bagnall D M. Fabrication and characterization of n-ZnO/p-AlGaIn heterojunction light-emitting diodes on 6H-SiC substrates. *Appl. Phys. Lett.* 2003; 83, 4719-4721.
- [62] Alivov Y I, Nostrand J E V, Look D C, Chukichev M V, Ataev B M. Observation of 430 nm electroluminescence from ZnO/GaN heterojunction light-emitting diodes. *Appl. Phys. Lett.* 2003; 83, 2943-2945.
- [63] Chichibu S F, Ohmori T, Shibata N, Koyama T, Onuma T. Fabrication of p-CuGaS₂/n-ZnO:Al heterojunction light-emitting diode grown by metalorganic vapor phase epitaxy and helicon-wave-excited-plasma sputtering methods. *J. Phys. Chem. Solids* 2005; 66, 1868-1871.
- [64] Xu S, Xu C, Liu Y, Hu Y F, Yang R S, Yang Q, Ryou J-H, Kim H J, Lochner Z, Choi S, Dupuis R, Wang Z L. Ordered nanowire array blue/near-UV light emitting diodes. *Adv. Mater.* 2010; 22, 4749-4753.
- [65] Bano N, Zaman S, Zainelabdin A, Hussain S, Hussain I, Nur O, Willander M. (2010), ZnO-organic hybrid white light emitting diodes grown on flexible plastic using low temperature aqueous chemical method. *J. Appl. Phys.* 2010; 108, 043103 (5 pages).
- [66] Guo Z, Zhang H, Zhao D X, Liu Y C, Yao B, Li B H, Zhang Z Z, Shen D Z. The ultralow driven current ultraviolet-blue light-emitting diode based on n-ZnO nanowires/i-polymer/p-GaN heterojunction. *Appl. Phys. Lett.* 2010; 97, 173508 (3 pages).
- [67] Alvi N H, Usman Ali S M, Hussain S, Nur O, Willander M. Fabrication and comparative optical characterization of n-ZnO nanostructures (nanowalls, nanorods, nanoflowers and nanotubes)/p-GaN white-light-emitting diodes. *Scripta Mater.* 2011; 64, 697-700.
- [68] Willander M, Nur O, Zaman S, Zainelabdin Z, Banon, Hussain I. (2011), Zinc oxide nanorods/polymer hybrid heterojunctions for white light emitting diodes. *J. Phys. D: Appl. Phys.* 2011; 44, 224017 (6 pages).

- [69] Zhang X M, Lu M-Y, Zhang Y, Chen L-J, Wang Z L. Fabrication of a high-brightness blue-light-emitting diode using a ZnO-nanowire array grown on p-GaN thin film. *Adv. Mater.* 2009; 21, 2767-2770.
- [70] Chang C-Y, Tsao F-C, Pan C-J, Chi G-C, Wang H-T, Chen J-J, Ren F, Norton D P, Pearson S J, Chen K-H, Chen L-C. Electroluminescence from ZnO nanowire/polymer composite p-n junction. *Appl. Phys. Lett.* 2006; 88, 173503 (3 pages)
- [71] Klason P, Rahman MM, Hu Q-H, Nur O, Turan R, Willander M. Fabrication and characterization of p-Si/n-ZnO heterostructured junctions. *Microelectronics Journal* 2009; 40, 706-710.
- [72] Lee S W, Cho H D, Panin G, Kang T W, Vertical ZnO nanorod/Si contact light-emitting diode. *Appl. Phys. Lett.* 2011; 98, 093110 (3 pages)
- [73] Park W I, Yi G C. Electroluminescence in n-ZnO nanorod arrays vertically grown on p-GaN. *Adv. Mater.* 2004; 16, 87-90.
- [74] Park S H, Kim S H, Han S W. Growth of homoepitaxial ZnO film on ZnO nanorods and light emitting diode applications. *Nanotech.* 2007; 18, 055608 (6 pages).
- [75] Lupan O, Pauporté T, Viana B. Low-voltage UV-electroluminescence from ZnO-nanowire array/p-GaN light-emitting diodes. *Adv. Mater.* 2010; 22, 3298-3302.
- [76] Zhang Q B, Guo H H, Feng Z F, Lin L L, Zhou J Z, Li Z H. n-ZnO nanorods/p-CuSCN heterojunction light-emitting diodes fabricated by electrochemical method. *Electrochim. Acta* 2010; 55, 4889 - 4894.
- [77] Xi Y Y, Hsu Y F, Djurišić A B, Ng A M C, Chan W K, Tam H L, Cheah K W. NiO/ZnO light emitting diodes by solution-based growth. *Appl. Phys. Lett.* 2008; 92, 113505 (3 pages).
- [78] Guo R, Nishimura J, Matsumoto M, Higashihata M, Nakamura D, Okada T. Electroluminescence from ZnO nanowire based p-GaN/n-ZnO heterojunction light-emitting diodes. *Appl. Phys. B, Photophys. Laser Chem.* 2009; 94, 33-38.
- [79] Mandalapu L J, Yang Z, Chu S, Liu J L. Ultraviolet emission from Sb-doped p-type ZnO based heterojunction light-emitting diodes. *Appl. Phys. Lett.* 2008; 92, 122101 (3 pages).
- [80] Li L, Yang Z, Kong J Y, Liu J L. Blue electroluminescence from ZnO based heterojunction diodes with CdZnO active layers. *Appl. Phys. Lett.* 2009; 95, 232117 (3 pages)
- [81] Nakahara K, Akasaka S, Yuji H, Tamura K, Fujii T, Nishimoto Y, Takamizu D, Sasaki A, Tanabe T, Takasu H, Amaike H, Onuma T, Chichibu S F, Sukazaki A, Ohtomo A, Kawasaki M. Nitrogen doped Mg_xZn_{1-x}O/ZnO single heterostructure ultraviolet-light-emitting diodes on ZnO substrates. *Appl. Phys. Lett.* 2010; 97, 013501 (3 pages).
- [82] Park T-Y, Choi Y-S, Kim S-M, Jung G-Y, Park S-J, Kwon B-J, Cho Y-H. Electroluminescence emission from light-emitting diode of p-ZnO/(InGa_xN_{1-x}/Ga_{1-x}N) multiquantum well/n-GaN. *Appl. Phys. Lett.* 2011; 98, 251111 (3 pages)

- [83] Sun J C, Feng Q J, Bian JM, Yu DQ, Li MK, Li CR, Liang HW, Zhao JZ, Qiu H, Du GT. Ultraviolet electroluminescence from ZnO-based light-emitting diode with p-ZnO:N/n-GaN:Si heterojunction structure. *J. Lumin.* 2011; 131, 825-828.
- [84] Hwang D-K, Kang S-H, Lim J-H, Yang E-J, Oh J-Y, Yang J-H, Park S-J. p-ZnO/n-GaN heterostructure ZnO light-emitting diodes. *Appl. Phys. Lett.* 2005; 86, 222101 (3 pages).
- [85] Choi H-K, Park J-H, Jeong S-H, Lee B-T. Realization of As-doped p-type ZnO thin films using sputter deposition. *Semicond. Sci. Technol.* 2009; 24, 105003 (4 pages).
- [86] Kim YY, Han WS, Cho HK. Determination of electrical types in the P-doped ZnO thin films by the control of ambient gas flow. *Appl. Surf. Sci.* 2010; 256, 4438-4441.
- [87] Kim HS, Lugo F, Pearton S J, Norton D P, Wang Y-L, Ren F. Phosphorus doped ZnO light emitting diodes fabricated via pulsed laser deposition. *Appl. Phys. Lett.* 2008; 92, 112108 (3 pages).
- [88] Tay C B, Chua S J, Loh K P. Stable p-type doping of ZnO film in aqueous solution at low temperatures. *J. Phys. Chem. C* 2010; 114, 9981-9987.
- [89] Wei ZP, Lu YM, Shen DZ, Zhang ZZ, Yao B, Li BH, Zhang JY, Zhao DX, Fan XW, Tang ZK. Room temperature p-n ZnO blue-violet light-emitting diodes. *Appl. Phys. Lett.* 2007; 90, 042113 (3 pages).
- [90] Chu S, Lim JH, Mandalapu LJ, Yang Z, Li L, Liu J L. (2008), Sb-doped p-ZnO/Ga-doped n-ZnO homojunction ultraviolet light emitting diodes. *Appl. Phys. Lett.* 2008; 92, 152103 (3 pages).
- [91] Kong JY, Chu S, Olmedo M, Li L, Yang Z, Liu J L. Dominant ultraviolet light emissions in packed ZnO columnar homojunction diodes. *Appl. Phys. Lett.* 2008; 93, 132113 (3 pages).
- [92] Liu W, Gu SL, Ye J D, Zhu SM, Liu S M, Zhou X, Zhang R, Shi Y, Zheng YD, Hang Y, Zhang CL. (2006), Blue-yellow ZnO homostructural light-emitting diode realized by metalorganic chemical vapor deposition technique. *Appl. Phys. Lett.* 2006; 88, 092101 (3 pages).
- [93] Sun J C, Zhao J Z, Liang H W, Bian J M, Hu L Z, Zhang H Q, Liang X P., Liu W F, Du GT. Realization of ultraviolet electroluminescence from ZnO homojunction with n-ZnO/p-ZnO:As/GaAs structure. *Appl. Phys. Lett.* 2007; 90, 121128 (3 pages).
- [94] Sun JC, Liang HW, Zhao JZ, Bian JM, Feng QJ, Hu LZ, Zhang HQ, Liang XP, Luo YM, Du GT. Ultraviolet electroluminescence from n-ZnO:Ga/p-ZnO:N homojunction device on sapphire substrate with p-type ZnO:N layer formed by annealing in N₂O plasma ambient. *Chem. Phys. Lett.* 2008; 460, 548-551.
- [95] Gu QL, Ling CC, Brauer G, Anwand W, Skorupa W, Hsu YF, Djurišić AB, Zhu CY, Fung S, Lu LW. Deep level defects in a nitrogen-implanted ZnO homogeneous p-n junction. *Appl. Phys. Lett.* 2008; 92, 222109 (3 pages).

- [96] Yang Y, Sun X. W, Tay B K, You G F, Tan S T, Teo KL. (2008), A p-n homojunction ZnO nanorod light-emitting diode formed by As ion implantation. *Appl. Phys. Lett.* 2008; 93, 253107 (3 pages).
- [97] Sun X W, Ling B, Zhao J L, Tan S T, Yang Y, Shen Y Q, Dong Z L, Li C X. Ultraviolet emission from a ZnO rod homojunction light-emitting diode. *Appl. Phys. Lett.* 2009; 95, 133124 (3 pages).
- [98] Lim J H, Kang C K, Kim K K, Park I K, Hwang D K, Park S J. UV electroluminescence emission from ZnO light-emitting diodes grown by high-temperature radio frequency sputtering. *Adv. Mater.* 2006; 18, 2720–2724.
- [99] Fang X, Li J H, Zhao D X, Shen D Z, Li B H, Wang X H. Phosphorus-doped p-type ZnO nanorods and ZnO nanorod p-n homojunction LED fabricated by hydrothermal method. *J. Phys. Chem. C* 2009; 113, 21208–21212.
- [100] Ryu Y R, Lee T-S, Lubguban J A, White H W, Kim B J, Park Y S, Youn C J. (2006), Next generation of oxide photonic devices: ZnO-based ultraviolet light emitting diodes. *Appl. Phys. Lett.* 2006; 88, 241108 (3 pages).